

**A CRITICAL ANALYSIS OF FATIGUE-CRACK  
PROPAGATION DATA FOR 2024-T3 ALUMINUM**

**Robert Alan Kish**

DUBLIN CITY LIBRARY  
GRADUATE SCHOOL  
DUBLIN, CALIFORNIA 93940

# NAVAL POSTGRADUATE SCHOOL

## Monterey, California



# THESIS

A CRITICAL ANALYSIS OF FATIGUE-CRACK  
PROPAGATION DATA FOR 2024-T3 ALUMINUM

by

Robert Alan Kish

December 1974

Thesis Advisor:

G.H. Lindsey

Approved for public release; distribution unlimited.

U164887



UNCLASSIFIED

SECURITY CLASSIFICATION OF THIS PAGE (When Data Entered)

| REPORT DOCUMENTATION PAGE  |                       | READ INSTRUCTIONS<br>BEFORE COMPLETING FORM                               |
|--|-----------------------|---|
| 1. REPORT NUMBER   | 2. GOVT ACCESSION NO. | 3. RECIPIENT'S CATALOG NUMBER   |
| 4. TITLE (and Subtitle)<br>A Critical Analysis of Fatigue-Crack Propagation Data for 2024-T3 Aluminum  |                       | 5. TYPE OF REPORT & PERIOD COVERED<br>Engineer's Thesis;<br>December 1974 |
|  |                       | 6. PERFORMING ORG. REPORT NUMBER  |
| 7. AUTHOR(s)<br>Robert Alan Kish   |                       | 8. CONTRACT OR GRANT NUMBER(s)  |
| 9. PERFORMING ORGANIZATION NAME AND ADDRESS<br>Naval Postgraduate School<br>Monterey, California 93940   |                       | 10. PROGRAM ELEMENT, PROJECT, TASK AREA & WORK UNIT NUMBERS               |
| 11. CONTROLLING OFFICE NAME AND ADDRESS<br>Naval Postgraduate School<br>Monterey, California 93940   |                       | 12. REPORT DATE<br>December 1974  |
|  |                       | 13. NUMBER OF PAGES<br>62   |
| 14. MONITORING AGENCY NAME & ADDRESS (if different from Controlling Office)<br>Naval Postgraduate School<br>Monterey, California 93940   |                       | 15. SECURITY CLASS. (of this report)<br>Unclassified                      |
|  |                       | 15a. DECLASSIFICATION/DOWNGRADING SCHEDULE                                |
| 16. DISTRIBUTION STATEMENT (of this Report)<br>Approved for public release; distribution unlimited.  |                       |   |
| 17. DISTRIBUTION STATEMENT (of the abstract entered in Block 20, if different from Report)   |                       |   |
| 18. SUPPLEMENTARY NOTES  |                       |   |
| 19. KEY WORDS (Continue on reverse side if necessary and identify by block number)<br>Fatigue prediction<br>Crack growth rate<br>Crack closure<br>Fatigue-crack growth data  |                       |   |
| 20. ABSTRACT (Continue on reverse side if necessary and identify by block number)<br>Fatigue-crack growth data for 2024-T3 aluminum was used to evaluate the accuracy of Forman's equation. Forman's equation was found to predict from one-third to twice the observed cycles to a given crack length when applied to multiple cyclic stress ratios. An alternative approach was developed, based on the observed data, which is applicable to analog or digital fatigue-crack growth prediction. Data acquisition based on |                       |   |

DD FORM 1473  
1 JAN 73  
(Page 1)EDITION OF 1 NOV 65 IS OBSOLETE  
S/N 0102-014-6601

UNCLASSIFIED

SECURITY CLASSIFICATION OF THIS PAGE (When Data Entered)



## (20. ABSTRACT Continued)

constant increment of crack length has been found to yield inadequate definition of the crack-growth curve in the low-cycle range for the successful application of the method. An expression was developed which extends the application of the crack-closure concept to the entire range of cyclic stress ratio. An effective root-mean-square stress was defined which shows indications of good correlation with the magnitude of the crack-growth curves.





A Critical Analysis of Fatigue-Crack  
Propagation Data for 2024-T3 Aluminum

by

Robert Alan Kish  
Lieutenant, United States Navy  
B.A., Arizona State University, 1967  
M.S., Naval Postgraduate School, 1974

Submitted in partial fulfillment of the  
requirements for the degree of

AERONAUTICAL ENGINEER

from the

NAVAL POSTGRADUATE SCHOOL  
December 1974



## ABSTRACT

Fatigue-crack growth data for 2024-T3 aluminum was used to evaluate the accuracy of Forman's equation. Forman's equation was found to predict from one-third to twice the observed cycles to a given crack length when applied to multiple cyclic stress ratios. An alternative approach was developed, based on the observed data, which is applicable to analog or digital fatigue-crack growth prediction. Data acquisition based on constant increment of crack length has been found to yield inadequate definition of the crack-growth curve in the low-cycle range for the successful application of the method. An expression was developed which extends the application of the crack-closure concept to the entire range of cyclic stress ratio. An effective root-mean-square stress was defined which shows indications of good correlation with the magnitude of the crack-growth curves.



## TABLE OF CONTENTS

|      |   |    |
|------|---|----|
| I.   | INTRODUCTION -----  | 11 |
| II.  | BACKGROUND -----  | 13 |
|      | A. MINER'S RULE OF CRACK INITIATION -----   | 13 |
|      | B. CRACK PROPAGATION -----  | 15 |
|      | C. STRESS INTENSITY FACTOR -----  | 16 |
|      | D. FORMAN'S EQUATION -----  | 17 |
|      | E. HUDSON'S DATA -----  | 18 |
| III. | DEVELOPMENT -----   | 20 |
|      | A. EVALUATION OF FORMAN'S EQUATION -----  | 20 |
|      | B. MATERIAL RESPONSE FUNCTION -----   | 23 |
|      | C. EFFECTIVE STRESS -----   | 26 |
|      | D. HYPERBOLIC REPRESENTATION OF<br>FATIGUE-CRACK GROWTH DATA -----  | 29 |
|      | E. NORMALIZATION OF THE DATA -----  | 31 |
| IV.  | CONCLUSIONS -----   | 34 |
| V.   | RECOMMENDATIONS FOR FUTURE RESEARCH -----   | 35 |
|      | APPENDIX A. INTEGRATION OF FORMAN'S EQUATION -----  | 36 |
|      | APPENDIX B. THE DERIVATION OF THE RELATIONSHIP<br>BETWEEN THE DAMAGE EFFECTIVE CYCLE<br>FRACTION AND THE CRACK-CLOSURE<br>PARAMETER ----- | 39 |
|      | LIST OF REFERENCES -----  | 61 |
|      | INITIAL DISTRIBUTION LIST -----   | 62 |



## LIST OF TABLES

|      |  |    |
|------|--|----|
| I.   | Fatigue-crack growth in 2024-T3 aluminum -----   | 43 |
| II.  | Analysis of the prediction accuracy of<br>Forman's equation for small cracks in<br>2024-T3 aluminum -----                      | 44 |
| III. | Coefficients, $d_1$ , resulting from the fit of<br>the fatigue-crack growth data to the general<br>second order equation ----- | 45 |





## LIST OF FIGURES

|     |  |    |
|-----|--|----|
| 1.  | Typical fatigue-crack growth curves (from Ref. 1) --   | 46 |
| 2.  | Hudson's comparison of fatigue-crack growth rate with Forman's equation (from Ref. 1) -----                                  | 47 |
| 3.  | Comparison of a fatigue-crack growth curve with the power-rule prediction (typical) -----                                    | 48 |
| 4.  | Comparison of fatigue-crack growth rate with Forman's equation for a single load case (typical) -                            | 49 |
| 5.  | Constant amplitude loading with crack closure -----  | 50 |
| 6.  | Schematic representation of the effect of increasingly negative cyclic stress ratios -----                                   | 51 |
| 7.  | Variation of the damage effective cycle fraction with cyclic stress ratio -----  | 52 |
| 8.  | Comparison of two expressions for the crack-closure parameter -----  | 53 |
| 9.  | Geometric interpretation of the general second order polynomial fit to the fatigue-crack growth data -----                   | 54 |
| 10. | Correlation of the coefficient $d_1^*$ with the effective RMS gross-section stress -----                                     | 55 |
| 11. | Correlation of the coefficient $d_2^*$ with the effective RMS gross-section stress -----                                     | 56 |
| 12. | Correlation of the coefficient $d_3^*$ with the effective RMS gross-section stress -----                                     | 57 |
| 13. | Correlation of the coefficient $d_4^*$ with the effective RMS gross-section stress -----                                     | 58 |
| 14. | Correlation of the coefficient $d_5^*$ with the effective RMS gross-section stress -----                                     | 59 |
| 15. | Relationship between the unstable crack propagation stress intensity factor and the effective RMS gross-section stress ----- | 60 |



## LIST OF SYMBOLS

### English

|                 |   |
|-----------------|---|
| a               | crack half-length   |
| f/T             | damage effective portion of a cycle or period   |
| K               | stress intensity factor   |
| K <sub>cr</sub> | value of the stress intensity factor in thin sheets which leads to unstable crack propagation under steady load |
| N               | cycles  |
| R               | cyclic stress ratio   |
| r               | radial coordinate referenced to the crack tip   |
| S               | gross-section stress  |
| T               | period of load application  |
| t               | time  |
| U               | crack closure parameter   |
| W               | specimen width  |
| x               | independent variable  |

### Greek

|                |  |
|----------------|--|
| $\Delta \dots$ | range of ...   |
| $\theta$       | angular coordinate measured from the line of crack advance |
| $\lambda$      | correlation factor   |
| $\sigma$       | local stress near the crack tip                            |
| $\omega$       | circular frequency of loading                              |



## Subscripts

|     |  |
|-----|--|
| a   | amplitude  |
| e   | effective  |
| i,j | tensor indices   |
| ins | instability, defining point of unstable crack propagation under unsteady loading |
| m   | mean   |
| max | maximum  |
| min | minimum  |
| op  | opening  |
| p   | predicted  |
| rms | root mean square   |
| w   | width  |



## ACKNOWLEDGEMENTS

The author wishes to express his appreciation to the Fatigue Section of the NASA Langley Research Center for the use of the fatigue-crack data examined in this thesis. Gratitude is extended to Assistant Professor G.H. Lindsey for his guidance and suggestions and to Barbara Kish for her patience and understanding.





## I. INTRODUCTION

Modern aircraft, particularly military aircraft, must be designed for high performance and long service life. The attempt to achieve higher performance in terms of increased payload, range, speed, or maneuverability implies a reduction in gross aircraft weight, or in the structural fraction of that weight. This constraint results in structural components which carry higher loads per unit area and places greater demands on their structural integrity.

The design values for the safe-life of non-inspectable components and the inspection intervals for other components are predicated upon the service life and the predicted load spectrum specified by the contracting agency. The aircraft components are sized to meet these design values using fatigue prediction techniques. The estimates of remaining life and maximum safe inspection intervals of operational aircraft are frequently re-evaluated in light of the operational load spectrum using similar methods. A factor of safety, or factor of uncertainty, is used in these calculations by which the expected life of a given structural configuration is reduced. This factor of safety (FS) directly reflects the accuracy of the prediction method used. Large FS, indicating poor accuracy, results in excessive structural weight when compared to the optimum and penalizes the aircraft performance throughout the service life.



Optimistic estimates of the accuracy of a method lead ultimately to costly retrofits and reduced aircraft availability. The long term economic efficiency of an aircraft is therefore dependent upon the accuracy of the fatigue prediction methods available to the designer and operator; thus considerable motivation exists for the improvement of fatigue life prediction accuracy.

The fail-safe design philosophy, which admits the existence of a crack in the structure, is one of the fatigue prediction approaches in current use. Crack growth predictions, in units of cycles from an initial size to its length when it precipitates catastrophic failure, are an essential element in the fatigue analysis of today's airplanes. Inspection periods and rework intervals can be prescribed from this information. This thesis reports an investigation of data and theory used widely, if not exclusively, in making crack growth predictions for aluminum alloys. Specifically, Hudson's fatigue crack growth data [1] for 2024-T3 aluminum alloy was examined in order to establish confidence limits on Forman's equation, which appears to be the most widely accepted crack growth prediction procedure used. Finally, an alternate method for expressing crack growth behavior is proposed to improve the accuracy of crack length predictions.



## II. BACKGROUND

The fatigue life of aircraft components is difficult to predict due to the many factors influencing the structural response to unsteady loading. These factors may be grouped into four categories; material characteristics, environmental effects, structural configuration, and service loading.

The fatigue response to unsteady loads is statistical in nature and is dependent upon the time history of the loading and material response, where material response is defined to be cycles to a given crack length. The response history may be divided into three stages. The first stage, termed crack initiation, is characterized by sub-microscopic cracks. This stage has been shown to be sensitive to a variety of microscopic damage mechanisms. The intermediate stage, termed crack propagation, is characterized by the relatively slow growth of a macroscopic crack (a few grain diameters) under the influence of the ordered external load. Final failure occupies a small fraction of the fatigue life of the material and a very high crack growth rate exists during this stage.

### A. MINER'S RULE OF CRACK INITIATION

The obvious complexity of the problem has led investigators to make certain simplifying assumptions and/or approximations. Miner [2] proposed a linear damage accumulation over the crack initiation stage of the fatigue life. This proposal defines



damage as the fraction of the initiation life in cycles,  $N_1$ , expended at the  $i^{\text{th}}$  load level. An increment of damage would then take place with each cycle at the  $i^{\text{th}}$  load level according to  $1/N_1$  or for  $n_1$  cycles, the damage would be  $n_1/N_1$ . Since the accumulation of damage was assumed to be linear, Miner's Rule predicts the fatigue life of a component as

$$L = \sum_i n_i \quad (1)$$

and damage as

$$D = \sum_i \frac{n_i}{N_1} \quad (2)$$

At the completion of the crack initiation stage,

$$\sum_i n_i/N_1 = 1 \quad (3)$$

Fatigue life data is presently available as  $S_a$  vs  $N_f$  curves where  $S_a$  is the alternating component of stress and  $N_f$  is the number of cycles to complete failure of the specimen rather than formation of a first crack. Application of Miner's rule to random load tests have yielded damage predictions at specimen failure considerably different from unity. Some refinements to Miner's approach to damage prediction have taken the form of weighting functions on each term or variable powers on each term such as  $D = \sum (n_i/N_1)^{m_i}$ .





These modifications as well as competing damage hypotheses have oftentimes resulted in improved prediction accuracy for a given set of data; however, the Miner summation of damage continues to be the most widely accepted due to its simplicity and the minimal improvement in accuracy offered by its more complicated alternatives.

## B. CRACK PROPAGATION

After the crack is formed, fail-safe design practice of crack-growth predictions requires a knowledge of the crack growth rate and the load under which the cracked structure would fail, both of which are not available from any damage theory. Many investigators, as summarized in Ref. 3, have attempted to correlate the crack growth per cycle to the gross section stress and the crack length, leading to propagation models of the form,

$$da/dN = f(S,a,\lambda) \quad (4)$$

where  $2a$  is the total crack length,  $S$  is the gross section stress and  $\lambda$  is a correction factor which compensates for finite width, rivet forces, etc. Paris and Erdogan [4] concluded that the stress intensity factor (SIF), which is a function of the same variables, was the parameter which best correlated with the crack growth rate observed.



### C. STRESS INTENSITY FACTOR

Mathematically, the stress intensity factors are undetermined coefficients arising from the solution of the field equations for any cracked geometry. The normal stress at the crack tip, under moderate static loading, is given by this solution as

$$\sigma_{ij} = \frac{K_1}{r^{1/2}} f_{ij}(\theta) + \frac{K_2}{r^{1/2}} g_{ij}(\theta) + \frac{K_3}{r^{1/2}} h_{ij}(\theta) \quad (5)$$

where  $K_1$ ,  $K_2$ , and  $K_3$  are the opening mode, in-plane shear mode, and out-of-plane shear mode SIF respectively,  $r$  is the radial coordinate referenced to the crack tip and  $\theta$  is the angular coordinate measured counter-clockwise from the advancing crack tip. The stress intensity factors may therefore be interpreted as parameters that reflect the redistribution of the stress field in a body resulting from the introduction of a crack. The magnitude of the stress intensity factor is dependent upon the geometry of the body containing the crack, the size and location of the crack, and distribution and magnitude of the external loads on the body. The configuration most readily treated is the sheet specimen containing a central crack of length  $2a$  under Mode I loading, for which

$$K_1 = S \lambda_w \sqrt{\pi a} \quad (6)$$



where  $\lambda_w$  is a width correction factor. The criterion for failure in the presence of a crack-like defect is that crack growth to failure (instability) will occur whenever the applied stresses,  $S$ , as given by equation (6) exceed some critical condition specified by  $K_I = K_{cr}$ . Paris and Ergodan [4] concluded from the preceding argument that this condition may be extended to fatigue and applied to the slow growth phase.

#### D. FORMAN'S EQUATION

Forman [5] proposed a model for crack propagation which utilized the range of the SIF as suggested by Paris [6],

$$\Delta K = K_{\max} - K_{\min} \quad (7)$$

to account for the cyclic loading typical of the fatigue environment. This model included the instability condition for failure as a singularity such that the growth rate approaches infinity as  $K_{\max}$  approaches  $K_{cr}$ . Forman's equation is written as

$$\frac{da}{dN} = \frac{C(\Delta K)^n}{(1-R)K_{cr} - \Delta K} \quad (8)$$

where  $C$  and  $n$  were assumed to be undetermined material constants and  $R$  is the ratio of minimum stress to maximum stress (loading ratio).



## E. HUDSON'S DATA

Hudson [1] conducted a most extensive study of the material response of two widely used aircraft alloys, 2024-T3 and 7075-T6 aluminum, to evaluate Forman's equation when applied to a large number of maximum stress conditions and loading ratio combinations. (The data obtained in Hudson's investigation was used as the data base for this study.)

The specimens used in Hudson's study were nominally 12 inches in width, 35 inches in length, and 0.090 inches in thickness. A notch 0.10 inches in length by 0.01 inches in width was cut into the center of each specimen by an electrical discharge machining technique. A reference grid of 0.050 inch spacing was photographically printed on the surface of each specimen to mark intervals in the path of the crack.

"Fatigue-crack growth was observed through 10-power microscopes while illuminating the specimen with stroboscopic light. The number of cycles required to propagate the crack to each grid line was recorded so that crack-propagation rates could be determined. Approximately two-thirds of the crack-propagation tests were conducted to failure. The remaining one-third were stopped before failure, and the cracked specimens were used in residual-static strength tests."<sup>1</sup>

---

<sup>1</sup>National Aeronautics and Space Administration Technical Note D-5390, Effect of Stress Ratio on Fatigue-Crack Growth in 7075-T6 and 2024-T3 Aluminum Alloy Specimens, by C. Michael Hudson, p. 5, August 1969.





The results of Hudson's fatigue-crack-growth tests on the 2024-T3 specimens are presented in Table I (reproduced from Ref. 1). Hudson obtained the fatigue-crack propagation rates graphically from the crack-growth curves defined in Table I. The crack-growth curves reproduced from Ref. 1 and shown as Figure 1 are typical. The results were presented as plots of the common logarithms of the experimental value of the crack-propagation rate as functions of the range of the SIF. Three models were then fitted to the data by least-squares techniques and compared to the data. Figure 2, from Ref. 1, is typical of the method used for the presentation of data and the evaluation of the quality of fit of empirical equations. Hudson concluded that Forman's equation produced an excellent fit for both materials whereas the other equations evaluated "...produced good correlation with the test data except at the high growth rates for the 7075-T6 alloy" on the basis of graphical representations of which Figure 2 is typical. This conclusion at first appears to be justified on the basis of plots such as Figure 2, however, the fatigue analyst is concerned with the accuracy with which a crack-propagation model predicts the number of cycles required for the crack to attain a given length. This is the basis upon which the fit should be evaluated.



### III. DEVELOPMENT

#### A. EVALUATION OF FORMAN'S EQUATION

Hudson used the tangent form of the width correction factor,

$$\lambda_w = \sqrt{\frac{W}{\pi a}} \tan \frac{\pi a}{W} \quad (9)$$

in evaluating the material constants, C and n, in Forman's equation. The differential equation resulting from the use of this form of width correction in Forman's equation may be integrated (Appendix A) using the small angle approximation,  $\tan \theta \approx \theta$ . This approximation is accurate to within three percent for crack lengths of less than 0.8 inches for Hudson's specimens.

The predicted interval of cycles between crack lengths,  $\Delta N_p$ , was calculated using Hudson's fit of Forman's equation and the integrated form of Forman's equation becomes

$$\Delta N_p = 2C_1 \left[ a_o^{\frac{2-n}{2}} \left( \frac{K_{cr}}{n-2} - \frac{S_{max} \sqrt{a_o}}{n-3} \right) - a^{\frac{2-n}{2}} \left( \frac{K_{cr}}{n-2} - \frac{S_{max} \sqrt{a}}{n-3} \right) \right] \quad (10)$$

where

$$C_1 = \frac{(1-R)}{C[(1-R)S_{max}]^n}$$



and  $\Delta N_p$  is the predicted number of cycles required to propagate at half-crack of length  $a_o$  to length  $a$ . The ratio of the predicted to the observed cycle increment is presented in Table II, where gross discrepancies exist for almost every case.

The load cases were also fitted individually in order to determine the cause of the poor predictions reported in Table II. The expression for  $\Delta K$  used in this analysis was

$$\Delta K = (S_{\max} - S_{\min}) \lambda_w \sqrt{\frac{a}{\pi}} \quad (11)$$

where Brown and Srawley's [7] finite width correction for a centrally cracked sheet,

$$\lambda_w = 1.77 + .277\left(\frac{2a}{W}\right) - .51\left(\frac{2a}{W}\right)^2 + 2.7\left(\frac{2a}{W}\right)^3, \quad (12)$$

was chosen on the basis of its reported accuracy. The test data for each load case were represented by a power series of the form

$$a = p_1 N^{e_1} + p_2 N^{e_2} + \dots + p_m N^{e_m} \quad (13)$$

which yields a very good approximation of the observed data as indicated by Figure 3. An analytic crack-growth rate expression was obtained by performing a differentiation of equation (13) with respect to cycles leading to



$$\frac{da}{dN} = p_1 e_1 N^{e_1-1} + p_2 e_2 N^{e_2-1} + \dots + p_m e_m N^{e_m-1} \quad (14)$$

Equations (11) and (13) were applied to each load case and a least-squares fit of Forman's equation to the data was performed. Figure 4 is typical of the individual fits thus obtained.

A regular, periodic variation of the calculated crack-growth rate about the fitted line was observed which is believed to indicate that Forman's equation may be an incorrect or incomplete functional form. These periodic variations appear as scatter when Forman's equation is called to fit multiple load cases. An apparent lower bound of crack-growth rate may also be observed in Figure 4. The failure of Forman's equation to represent this threshold level probably accounts for the largest portion of prediction error. Just as for the integration performed for Hudson's fit, consistent prediction errors were noted for the fits of the individual load cases but of smaller magnitude. The periodic variation of the data about the fitted line and the apparent lower threshold of crack-growth rate led to the development of a new material response model. Equation (13) was not considered to be a practical alternative to Forman's equation in view of the explicit appearance of the variable  $N$ , which is unknown in the practical application of any prediction model. Series reversion was likewise discounted due to non-integer exponents resulting from the fit.





## B. MATERIAL RESPONSE FUNCTION

A material response function was developed in which the response was assumed to be a piecewise continuous function of time, loading conditions, and crack geometry. The function was also assumed to possess piecewise continuous time derivatives. This assumption was based on the satisfactory representation of the data achieved by the power series approximation of the fatigue data, equation (13), which has an infinite number of continuous time derivatives.

Previous investigators have assumed that the fatigue-crack propagation rate,  $da/dN$ , has the functional form

$$da/dN = f(S(N), a(N), \lambda(N)) \quad (15)$$

where the variables have the meanings previously defined and are functions of time or, alternatively, cycles. Although the relationship between the independent variables  $N$  and  $t$  is linear, as expressed by

$$N = \omega t \quad (16)$$

where  $\omega$  is the circular frequency of loading, a distinction in the growth rates  $da/dt$  and  $da/dN$  exists. The crack-growth rate  $da/dt$  is an instantaneous rate which must be integrated over the period of a cycle in order to obtain the time average rate,  $da/dN$ .



Paris [6] concluded that the crack growth rate was best represented as a function of the range SIF as given by equation (11). The desired function must predict crack growth rate under constant amplitude and random loading with equal precision since constant amplitude loading is a special case of random loading. The stress range is therefore a constant for either load case taken on a cycle-by-cycle basis. This argument applies equally well to any other choice of the characteristic stress to be used in calculating the SIF. The expression for crack-growth rate could then be represented equally well by the functional form

$$\frac{da}{dN} = f_1(a(N), \lambda_w(N)) \quad (17)$$

or

$$\frac{da}{dN} = f_2(x(N)) \quad (18)$$

where

$$x = \lambda_w(a, W) \sqrt{a(N)}$$

since  $\lambda$  is a function of crack geometry only.

Introduction of the requirement for higher order derivatives can be satisfied by a linear summation of the assumed form

$$x = c_1 \frac{dx}{dN} + c_2 \frac{d^2x}{dN^2} + \dots + c_k \frac{d^kx}{dN^k} \quad (19)$$



where the  $c_1 = c_1(S)$ . Equation (19) is a linear differential equation in  $N$  with constant coefficients and thus has a solution of exponential functions. Paris [6] noted that the crack growth rate is a monotonically increasing function of the stress intensity factor. The crack length,  $a$ , increases monotonically with time and the width correction,  $\lambda$ , increases monotonically with crack length, therefore the rate of change of the variable,  $x$ , with respect to cycles (time) must increase monotonically with  $x$ . This type of response is typical of positive feedback systems, which implies that the roots of the characteristic equation obtained from equation (19) are real. A mathematical model of the desired material response function is therefore the Prony series

$$x = \sum_i b_{2i-1} \exp[b_{2i}N] \quad (20)$$

which satisfies all requirements heretofore set forth.

This form of the material response function may be recast to the differential

$$\frac{d^k x}{dN^k} = \frac{1}{c_k} \left[ c_1 \frac{dx}{dN} + c_2 \frac{d^2 x}{dN^2} + \dots + c_{k-1} \frac{d^{k-1} x}{dN^{k-1}} - x \right] \quad (21)$$

when the functional form of the  $c_1$  is determined. This differential equation would find utility if programmed for analog or hybrid computation using non-linear elements



eliminating the excessive digital computer time requirements typical of random loading fatigue calculations; however, it is beyond the scope of this thesis. This approach to fatigue prediction calculations would also allow the use of discretized flight load data without intermediate processing.

The data sampling frequency used by Hudson, based on equal increments of crack length, provided insufficient data in the low cycle range of the specimen lives. The crack growth rate progresses from a nearly constant value at small crack lengths to much larger values within a small increment of crack length requiring a more frequent data sampling frequency in order to achieve a successful analysis of the exponential form of the fatigue response function through direct analysis.

### C. EFFECTIVE STRESS

The extension of equation (20) to account for random load sequences requires that the constants be a function of the loading conditions. The representation of the piecewise continuous response function,  $x'(t)$ , as the cycle average function  $x(N)$  leads to the representation of the piecewise continuous crack-growth rate,  $da(t)/dt$ , as the time average crack-growth rate,  $da(N)/dN$ . Consistency requires that the loading also be represented as a time average variable. Paris [16] suggested the utility of the Root-Mean-Square (rms) gross section stress, as defined as





$$S_{rms}^2 = \frac{1}{T} \int_0^T S^2(t) dt \quad (22)$$

where  $S(t) = S_m + S_a \sin \omega t$

and  $S_m$  is the mean gross section stress during the cycle,  $S_a$  is the amplitude of the gross section varying stress during the cycle,  $\omega$  is the circular frequency and  $T$  is the period of the cycle.

The entire magnitude of the stress described above does not contribute to crack propagation. Elber [8] has noted that plastic yielding at the crack tip results in a compressive residual stress upon unloading. This compressive stress at the crack tip delays the opening of the crack. Elber defined the crack closure parameter,  $U$ , as

$$U = \frac{S_{max} - S_{op}}{S_{max} - S_{min}} \quad (23)$$

where  $S_{op}$  is the gross section stress at which the crack opens. He found that  $U$  seemed to be a linear function of loading ratio for 2024-T3 aluminum as represented by

$$U = 0.4R + 0.5 \quad (24)$$

Since no crack propagation occurs while the crack is closed, an effective rms gross section stress may be defined as



$$S_{rms}^2 = \int_0^1 S_e^2 \frac{dt}{T} \quad (25)$$

where  $S_e = S_m + S_a \sin \frac{2\pi t}{T} - S_{op}$

subject to  $S_e \geq 0$ .

The nature of the sinusoidal function is such that the limits of integration can be shifted to write (25) more conveniently in terms of the damage effective portion of the cycle as illustrated in Figure 5. This leads to

$$S_{rms_e}^2 = \int_{\frac{1}{4} - \frac{f}{2T}}^{\frac{1}{4} + \frac{f}{2T}} S_e^2 \frac{dt}{T} + \int_{\frac{1}{4} + \frac{f}{2T}}^{\frac{1}{4} - \frac{f}{2T}} 0 \frac{dt}{T} \quad (26)$$

where  $f/T$  is the fraction of the cycle during which the crack is open and is defined by (See Appendix B)

$$f/T \triangleq \frac{\cos^{-1}(1-2U)}{\pi} \quad (27)$$

Elber's equation for  $U(R)$  leads to effective cycle fractions which are undefined for load ratios less than -1.25. This unnatural behavior in the neighborhood of a subset of Hudson's data motivated a search for a more satisfactory representation of the crack closure phenomenon. Figure 7 is a schematic of the loading conditions for increasingly negative load ratios. Reasoning from this figure indicates that, in the limit, as  $S_{max}$  approaches zero ( $R$  approaches



negative infinity), the fraction of the period over which the crack is open approaches zero. This physical constraint is satisfied by an equation of the form

$$\frac{f}{T} = \frac{A}{B - R} \quad (28)$$

where A and B were assumed to be undetermined material constants. Substitution of equation (28) into the definition of  $f/T$ , equation (27), leads to

$$U = \frac{1}{2} [1 - \cos \pi (\frac{A}{B - R})] \quad (29)$$

Elber's data [8] was fitted to the function for the effective cycle fraction, equation (28), as shown in Figure 6. The form satisfies the physical constraint and yields a smaller  $\chi^2$  error than equation (24) when compared in Figure 7. Figure 7 is a comparison of the functional representation of  $U(R)$  as developed in this study with that of Elber. Both forms appear to be incomplete in that neither form considers the effects of absolute load level or crack geometry on the crack closure phenomenon.  $S_{rms_e}$  was calculated on the basis of equations (25) and (28).

#### D. HYPERBOLIC REPRESENTATION OF FATIGUE-CRACK GROWTH DATA

On the basis of the arguments presented with regard to the exponential form of the material response function and the observed similarity of the exponential and hyperbolic



curve forms, Hudson's fatigue-crack growth data was fitted to the general form of the second order equation,

$$Ax^2 + BxN + CN^2 + Dx + EN = 1 \quad (30)$$

Solving for N, Table III is a listing of the coefficients of the equation

$$N = d_1x + d_2 \pm \sqrt{d_3x^2 + d_4x + d_5} \quad , \quad (31)$$

ordered with decreasing  $S_{rms}$ , which resulted from the fit of equation (30).

Figure 8 indicates the quality typical of these coefficients. The variation in sign which occurs in Table III reflects both the translation of the x axis (or the N ordinate of the center of the fitted hyperbola) and the frequent occurrence of parabolic, rather than hyperbolic, coefficients. The parabolic coefficients (sign of A = sign of C in equation (30)) resulted from the paucity of data in the low-cycle range of the specimen fatigue life. The appearance of parabolic coefficients is unacceptable from a physical standpoint as the parabolic form implies that cycles to a given crack length is not a single valued function, as shown schematically in Figure 9a. The translation of the center of the assumed hyperbola was an unavoidable result of the presence of the original machined





notch. Figure 9b is a schematic representation of the effect of load level and the presence of the artificial notch on the translation of the x axis.

#### E. NORMALIZATION OF THE DATA

A unified fatigue prediction method may be formulated by combining the capabilities of the damage accumulation method in estimating crack initiation with the fracture mechanics approach applied over the crack propagation and failure stages. This usage demands the normalization of all load cases to a common reference crack length which should be the minimum detectable crack length defining initiation. This normalization was accomplished for each (hyperbolic) load case by estimating the cyclic interval between Hudson's reference point, typically 0.10 inch, and the assumed initiation points, 0.003 inch. The estimate was made on the basis of equation (31) using the  $d_i$  previously calculated and was then applied as an increment to the observed cycles to a given crack length for an unnotched specimen. The modified data sets were again fit to equation (30) yielding estimated coefficients,  $d_i^*$ , of the unnotched sheet which are hypothesized to correlate with  $S_{rms_e}$ . Figures 10 through 14 indicate the degree of this correlation and suggest that the appropriate functional relation may be

$$d_i^* = \alpha_i S_{rms_e}^{\beta_i} \quad (32)$$



An analytic expression for the crack-growth rate,  $da/dN$ , may be obtained by the chain differentiation

$$\frac{da}{dN} = \frac{da}{dx} \frac{dx}{dN} = \frac{1}{\left(\frac{dx}{da}\right)} \frac{1}{\left(\frac{dN}{dx}\right)} \quad (33)$$

$$\text{where } \frac{dx}{da} = \frac{1}{a} \left( \frac{\lambda}{2} + a \frac{d\lambda}{da} \right) \quad (34)$$

$$\text{and } \frac{dN}{da} = d_1 - \frac{\frac{1}{2} (2d_3x + d_4)}{\sqrt{d_3x^2 + d_4x + d_5}} \quad (35)$$

This expression for  $da/dN$  approaches the constant (threshold) crack-growth rate observed in Figure 4 at small crack lengths and satisfies the instability condition given that equation (34) has a zero.

The zero of equation (34) yields  $x_{ins}$  and leads to

$$K_{ins} = S_{max} x_{ins} \quad (36)$$

where the instability condition has been assumed to take place at the instant in the last cycle at which the load has attained its maximum value. Figure 15 depicts the variation of the ratio  $K_{ins}/K_{cr}$ . This apparent reduction of the level of the stress intensity factor for unstable crack



propagation is attributed to dynamic effects on propagation and has the effect of minimizing the influence of the singularity condition in Forman's equation.

The data fits to equation (30) yielded no real solution to equation (34) for some load cases. These load cases appeared to be the dynamic tests which were terminated well before failure and therefore contained insufficient information regarding the shape of the response function in the high-cycle region to give the correct physical response.



#### IV. CONCLUSIONS

Hudson's [1] fatigue-crack growth data for 2024-T3 aluminum was used to evaluate the accuracy of Forman's equation. An alternative approach to the representation of the propagation process was developed and analyzed. An expression was developed which extends Elber's crack-closure concept to the possible load ratio range. The following conclusions can be drawn from this study.

1. Forman's equation does not appear to satisfactorily predict crack propagation in 2024-T3 when evaluated on the basis of the observed data.

2. Elber's crack-closure concept was successfully extended to the entire load ratio range in 2024-T3 by the relation

$$U = \sin^2 \left( \frac{.526}{2.169 - R} \right)$$

3. The development of a crack-growth rate expression based on empirical analysis of the observed data met with limited success due to the coarse data resolution in the low-cycle range.

4. The stress intensity factor at crack instability under dynamic loading conditions was observed to decrease with decreasing values of effective rms gross-section stress, asymptotically approaching a value of approximately one-third the value measured under static loading.





#### IV. RECOMMENDATIONS FOR FUTURE RESEARCH

The material response of 2024-T3 aluminum has been shown to be capable of representation by a continuous response function. The accumulation of a number of test sets with more frequent data sampling in the low-cycle phase of the crack propagation life would allow a determination of a material response model for which statistical reliability limits could be determined. Any such model must be based upon the observed data, as compared to derived data, for the reliability limits to be meaningful.

The development of the exponential response model will allow the determination of the governing differential equation for crack propagation under dynamic loading by the application of parameter identification techniques. Such a development would allow the calculation of the expected crack length under random loading by the use of analog, rather than digital, computation devices.



## APPENDIX A. INTEGRATION OF FORMAN'S EQUATION

Forman's equation is written

$$\frac{da}{dN} = \frac{C(\Delta K)^n}{(1-R)K_{cr} - \Delta K} \quad (A-1)$$

where the stress intensity factor,  $K$ , is defined as

$$K \triangleq S\lambda\sqrt{\pi a} \quad (A-2)$$

and the range of the stress intensity factor is written

$$\Delta K = \Delta S\lambda\sqrt{\pi a} \quad (A-3)$$

The tangent form of the width correction factor,

$$\lambda_w = \sqrt{\frac{W}{\pi a} \tan \frac{\pi a}{W}} \quad (A-4)$$

may be used, allowing the small angle approximation. This approximation,  $\tan \theta = \theta$ , yields errors of less than three percent for ratios of crack half-length to width of less than 1/15.

Limiting the integration to this range allows  $\Delta K$  to be expressed as

$$\Delta K = \Delta S\sqrt{a} \quad (A-5)$$



The cyclic stress ratio, R, is defined

$$R = \frac{S_{\max}}{S_{\min}} \quad (\text{A-6})$$

$$\text{Therefore } \Delta S = (1-R)S_{\max} \quad (\text{A-7})$$

Forman's equation can be rewritten as

$$\frac{da}{dN} = \frac{C(1-R)^n S_{\max}^n a^{n/2}}{(1-R)K_{cr} - S_{\max} a^{1/2}} \quad (\text{A-8})$$

for the limitations imposed.

Treating this expression as a differential as proposed by Forman [5]

$$dN = \frac{(1-R)(K_{cr} - S_{\max} a^{1/2})}{C(1-R)^n S_{\max}^n a^{1/2}} da \quad (\text{A-9})$$

which may be integrated between crack half-lengths  $a_0$  and  $a$

$$\Delta N_p = \frac{(1-R)}{C(1-R)^n S_{\max}^n} \int_{a_0}^a \frac{K_{cr} - S_{\max} a^{1/2}}{a^{n/2}} da \quad (\text{A-10})$$

Carrying out the indicated integration yields

$$\Delta N_p = \frac{(1-R)}{C(1-R)^n S_{\max}^n} \left[ \frac{K_{cr} a^{\frac{2-n}{2}}}{\frac{2-n}{2}} - \frac{S_{\max} a^{\frac{3-n}{2}}}{\frac{3-n}{2}} \right]_{a_0}^a \quad (\text{A-11})$$



Simplification of equation (A-11) leads to

$$\Delta N_p = 2C_1 \left[ a_o^{\frac{2-n}{2}} \frac{K_{cr}}{n-2} - \frac{S_{max} \sqrt{a_o}}{n-3} - a^{\frac{2-n}{2}} \frac{K_{cr}}{n-2} - \frac{S_{max} \sqrt{a}}{n-3} \right] \quad (A-12)$$

where

$$C_1 = \frac{(1-R)}{C(1-R)^n S_{max}^n} \quad (A-13)$$

and  $\Delta N_p$  is the cyclic increment predicted to elapse during the extension of a crack of half-length  $a_o$  to a half-length of  $a$  when subjected to constant amplitude loading conditions  $R$  and  $S_{max}$ .





APPENDIX B. THE DERIVATION OF THE RELATIONSHIP BETWEEN  
THE DAMAGE EFFECTIVE CYCLE FRACTION AND  
THE CRACK-CLOSURE PARAMETER

Crack propagation occurs only when the fatigue crack is open, allowing the definition of a damage effective portion of a cycle (period). This fraction of the period is bounded by the limits  $t_1/T$  and  $t_2/T$  representing the instants of crack opening and crack closing, respectively. The damage effective fraction is then

$$f/T = t_2/T - t_1/T \quad (B-1)$$

These limits are symmetric about the maximum load instant for constant amplitude loading. Assuming a loading function of the form

$$S(t/T) = S_m + S_a \sin (2\pi t/T) \quad (B-2)$$

the limits of the damage effective fraction of the cycle may be written

$$t_1/T = 1/4 - f/(2T) \quad (B-3a)$$

and

$$t_2/T = 1/4 + f/(2T) \quad (B-3b)$$



The crack opens during the loading portion of the period when the effective gross section stress is zero. The crack-closure concept modifies this stress by the inclusion of the residual stresses resulting from local tensile yielding at the crack tip. Defining  $S_{op}$  to be the gross section stress at which the crack opens leads to

$$S_e(t/T) = S_m - S_{op} + S_a \sin(2\pi t/T) \quad (B-4)$$

The instant of crack opening is therefore defined by

$$S_e(t_1/T) = S_m - S_{op} + S_a \sin(2\pi t_1/T) \equiv 0 \quad (B-5)$$

or

$$\left(\frac{S_{op} - S_m}{S_a}\right) = \sin[2\pi(1/4 - f/2T)] \quad (B-6)$$

Trigonometric reduction yields

$$\left(\frac{S_{op} - S_m}{S_a}\right) = \cos(\pi f/T) \quad (B-7)$$

and the damage effective fraction of the cycle is defined in terms of the loading and closure parameters

$$f/T \triangleq \cos^{-1}/\pi \left(\frac{S_{op} - S_m}{S_a}\right) \quad (B-8)$$



Rewriting Equation (B-8) in terms of  $S_{\max}$  and  $S_{\min}$  yields

$$f/T = \cos^{-1}/\pi \left[ \frac{S_{op} - \left( \frac{S_{\max} + S_{\min}}{2} \right)}{\left( \frac{S_{\max} - S_{\min}}{2} \right)} \right] \quad (B-9)$$

which simplifies to

$$f/T = \cos^{-1}/\pi \left[ 1 - \frac{2(S_{\max} - S_{op})}{S_{\max} - S_{\min}} \right] \quad (B-10)$$

This becomes

$$f/T = \cos^{-1}/\pi [1 - 2U] \quad (B-11)$$

with Elber's [8] definition of the crack-closure parameter,  $U$ ,

$$U = \frac{S_{\max} - S_{op}}{S_{\max} - S_{\min}} \quad (B-12)$$

Solving Equation (B-12) for  $U$  yields

$$U = \frac{1}{2} (1 - \cos \pi f/T) \quad (B-13)$$

Therefore, the relation between  $f/T$  and  $U$  is

$$U = \sin^2 \left( \frac{\pi f}{2T} \right) \quad (B-14)$$



and

$$f/T = 2/\pi \sin^{-1} (U)^{\frac{1}{2}} \quad (B-15)$$





TABLE I. Fatigue-crack growth in 2024-T3 aluminum (from Ref. 1).

| $S_m$ |                   | $S_a$ |                   | Loading frequency<br>Hz | Nominal<br>R value | Average number of cycles required to propagate a crack from a half-length $a$ of 0.10 in. (2.54 mm) to a half-length $a$ of - |                       |                        |                        |                        |                        |                        |                        |                        |                        |                        |
|-------|-------------------|-------|-------------------|-------------------------|--------------------|---|-----------------------|------------------------|------------------------|------------------------|------------------------|------------------------|------------------------|------------------------|------------------------|------------------------|
| ksi   | N/mm <sup>2</sup> | ksi   | N/mm <sup>2</sup> |                         |                    | 0.20 in.<br>(5.08 mm)   | 0.30 in.<br>(7.62 mm) | 0.40 in.<br>(10.16 mm) | 0.50 in.<br>(12.70 mm) | 0.70 in.<br>(17.78 mm) | 0.80 in.<br>(20.32 mm) | 0.90 in.<br>(22.86 mm) | 1.00 in.<br>(25.40 mm) | 1.20 in.<br>(30.48 mm) | 1.40 in.<br>(35.58 mm) | 1.60 in.<br>(40.64 mm) |
| 0     | 0                 | 25    | 172               | 30                      | 0.5                | -1  | 3 300                 | 3 700                  | 3 950                  | 4 100                  | 4 200                  | 4 280                  | 4 330                  | 4 370                  |                        |                        |
| 0     | 0                 | 20    | 138               | 30                      | 0.5                | -1  | 0 900                 | 8 100                  | 8 900                  | 9 400                  | 9 750                  | 10 000                 | 10 150                 | 10 300                 |                        |                        |
| 0     | 0                 | 15    | 103               | 820                     | 13.7               | -1  | 26 500                | 32 000                 | 35 800                 |                        |                        |                        |                        |                        |                        |                        |
| 0     | 0                 | 10    | 69                | 820                     | 13.7               | -1  | 89 000                | 105 000                | 117 000                | 127 000                | 130 000                | 143 000                | 148 000                | 153 000                |                        |                        |
| 0     | 0                 | 0     | 0                 | 820                     | 13.7               | -1  | 90 000                | 140 000                | 170 000                | 195 000                | 210 000                | 225 000                | 240 000                | 250 000                | 285 000                |                        |
| 15    | 103               | 15    | 103               | 20                      | 0.3                | 0   | 3 900                 | 4 400                  | 4 700                  | 4 850                  | 5 000                  |                        |                        |                        |                        |                        |
| 10    | 69                | 10    | 69                | 1200                    | 20.0               | 0   | 9 000                 | 19 500                 | 22 000                 | 23 500                 | 24 300                 | 25 000                 | 25 300                 |                        |                        |                        |
| 7.5   | 52                | 7.5   | 52                | 1200                    | 20.0               | 0   | 24 000                | 46 500                 | 53 000                 | 58 500                 | 62 500                 | 85 500                 | 87 500                 | 69 000                 | 71 500                 |                        |
| 5     | 34                | 5     | 34                | 1200                    | 20.0               | 0   | 142 000               | 200 000                | 210 000                | 228 000                | 239 000                | 248 000                | 256 000                | 282 000                | 274 000                | 288 000                |
| 3.75  | 26                | 3.75  | 26                | 1800                    | 30.0               | 0   | 610 000               | 780 000                | 840 000                | 880 000                | 910 000                | 950 000                | 970 000                | 980 000                | 1 010 000              | 1 030 000              |
| 20    | 138               | 10    | 69                | 1200                    | 20.0               | .33   | 8 800                 | 10 200                 | 10 900                 |                        |                        |                        |                        |                        |                        |                        |
| 15    | 103               | 7.5   | 52                | 1200                    | 20.0               | .33   | 12 000                | 22 700                 | 25 500                 | 27 500                 | 28 800                 | 29 800                 | 30 500                 | 31 100                 |                        |                        |
| 12.5  | 86                | 6.3   | 43                | 1200                    | 20.0               | .33   | 20 500                | 39 000                 | 44 000                 | 47 000                 | 50 000                 | 52 000                 | 53 500                 | 55 000                 |                        |                        |
| 10    | 69                | 5     | 34                | 1200                    | 20.0               | .33   | 60 000                | 95 000                 | 101 700                | 115 000                | 120 000                | 125 000                | 130 000                | 132 000                | 137 000                | 142 000                |
| 5     | 34                | 2.5   | 17                | 1800                    | 30.0               | .33   | 550 000               | 780 000                | 900 000                | 1 000 000              | 1 050 000              | 1 090 000              | 1 150 000              | 1 170 000              | 1 220 000              | 1 240 000              |
| 2.5   | 155               | 7.5   | 52                | 1200                    | 20.0               | .5  | 9 500                 | 16 500                 | 18 000                 | 18 800                 | 19 200                 |                        |                        |                        |                        |                        |
| 15.75 | 129               | 8.25  | 43                | 1200                    | 20.0               | .5  | 18 500                | 32 500                 | 35 600                 | 38 200                 | 40 000                 | 41 000                 | 42 100                 | 42 800                 |                        |                        |
| 15    | 103               | 5     | 34                | 1200                    | 20.0               | .5  | 29 000                | 43 000                 | 51 000                 | 62 000                 | 66 000                 | 69 000                 | 71 000                 | 73 000                 | 75 000                 | 76 000                 |
| 11.25 | 78                | 3.75  | 26                | 1200                    | 20.0               | .5  | 165 000               | 213 000                | 238 000                | 255 000                | 270 000                | 280 000                | 289 000                | 303 000                | 312 000                | 318 000                |
| 7.5   | 52                | 2.5   | 17                | 1800                    | 30.0               | .5  | 1 100 000             | 1 670 000              | 1 870 000              | 1 930 000              | 1 980 000              | 2 020 000              | 2 050 000              | 2 100 000              | 2 130 000              | 2 160 000              |
| 30    | 207               | 5     | 34                | 820                     | 13.7               | .7  | 51 000                | 67 000                 | 73 000                 | 77 000                 |                        |                        |                        |                        |                        |                        |
| 25    | 172               | 4.4   | 30                | 820                     | 13.7               | .7  | 84 000                | 107 000                | 119 000                | 126 000                |                        |                        |                        |                        |                        |                        |
| 20    | 138               | 3.5   | 24                | 820                     | 13.7               | .7  | 248 000               | 296 000                | 322 000                | 338 000                | 350 000                | 359 000                | 380 000                | 370 000                |                        |                        |
| 15    | 103               | 2.6   | 18                | 820                     | 13.7               | .7  | 590 000               | 810 000                | 890 000                | 940 000                | 970 000                | 1 000 000              | 1 020 000              | 1 040 000              | 1 070 000              | 1 090 000              |
| 10    | 69                | 1.7   | 12                | 820                     | 13.7               | .7  |                       | 1 000 000              | 1 500 000              | 1 750 000              | 1 890 000              | 2 000 000              | 2 070 000              | 2 150 000              | 2 210 000              | 2 250 000              |

<sup>a</sup> Except as noted.

<sup>b</sup> Crack was initiated and propagated to  $a = 0.15$  inch (3.8 mm) at  $S_a = 10$  ksi (69 MN/m<sup>2</sup>) to expedite testing; cycles listed are number required to propagate crack from  $a = 0.20$  inch (5.08 mm).

<sup>c</sup> Crack was initiated and propagated to  $a = 0.18$  inch (4.6 mm) at  $S_a = 5$  ksi (34 MN/m<sup>2</sup>) to expedite testing; cycles listed are number required to propagate crack from  $a = 0.30$  inch (7.62 mm).



TABLE II. Analysis of the prediction accuracy of Forman's equation for small cracks in 2024-T3 aluminum.

| S <sub>m</sub><br>ksi | S <sub>a</sub><br>ksi | Nominal<br>R value | Ratio of cycles predicted to cycles<br>observed for propagation from a=0.10 inch |      |      |      |      |      |      |
|-----------------------|-----------------------|--------------------|--|------|------|------|------|------|------|
|                       |                       |                    | to.2   | .3   | .4   | .5   | .6   | .7   | .8   |
| 0                     | 25                    | -1                 | .44  | .43  | .44  | .44  | .45  | .45  | .46  |
| 0                     | 20                    | -1                 | .47  | .46  | .45  | .44  | .44  | .44  | .44  |
| 0                     | 15                    | -1                 | .36  | .33  | .31  | .30  |      |      |      |
| 0                     | 10                    | -1                 | .43  | .40  | .39  | .38  | .37  | .36  | .36  |
| 0                     | 7.5                   | -1                 |  | .30  | .30  | .30  | .30  | .30  | .30  |
|                       |                       |                    |  |      |      |      |      |      |      |
| 15                    | 15                    | 0                  | 1.00   | .98  | .99  | 1.00 | 1.01 | 1.01 |      |
| 10                    | 10                    | 0                  | 1.32   | 1.08 | .97  | .93  | .91  | .91  | .91  |
| 7.5                   | 7.5                   | 0                  | 1.36   | 1.21 | 1.12 | 1.07 | 1.02 | .99  | .97  |
| 5                     | 5                     | 0                  | .94  | 1.04 | 1.07 | 1.08 | 1.08 | 1.07 | 1.06 |
| 3.75                  | 3.75                  | 0                  | .59  | .64  | .69  | .71  | .73  | .74  | .75  |
|                       |                       |                    |  |      |      |      |      |      |      |
| 20                    | 10                    | .33                | 1.21   | 1.14 | 1.12 | 1.13 |      |      |      |
| 15                    | 7.5                   | .33                | 1.72   | 1.55 | 1.43 | 1.38 | 1.34 | 1.32 | 1.31 |
| 12.5                  | 6.3                   | .33                | 1.88   | 1.69 | 1.56 | 1.50 | 1.47 | 1.44 | 1.42 |
| 10                    | 5                     | .33                | 1.43   | 1.45 | 1.44 | 1.46 | 1.36 | 1.35 | 1.33 |
| 5                     | 2.5                   | .33                | 1.72   | 1.69 | 1.69 | 1.65 | 1.66 | 1.66 | 1.66 |
|                       |                       |                    |  |      |      |      |      |      |      |
| 22.5                  | 7.5                   | .5                 | 1.54   | 1.42 | 1.38 | 1.36 | 1.36 | 1.37 |      |
| 18.75                 | 6.25                  | .5                 | 1.52   | 1.40 | 1.36 | 1.34 | 1.31 | 1.29 | 1.29 |
| 15                    | 5                     | .5                 | 2.14   | 1.99 | 1.93 | 1.86 | 1.80 |      |      |
| 11.25                 | 3.75                  | .5                 | 1.03   | 1.11 | 1.14 | 1.15 | 1.15 | 1.15 | 1.14 |
| 7.5                   | 2.5                   | .5                 | .63  | .58  | .60  | .63  | .64  | .66  |      |
|                       |                       |                    |  |      |      |      |      |      |      |
| 30                    | 5                     | .7                 | .62  | .64  | .66  | .68  |      |      |      |
| 25                    | 4.4                   | .7                 | .63  | .68  | .70  | .71  |      |      |      |
| 20                    | 3.5                   | .7                 | .49  | .56  | .59  | .60  | .61  | .62  | .62  |
| 15                    | 2.6                   | .7                 | .58  | .58  | .58  | .61  | .62  | .63  | .64  |
| 10                    | 1.7                   | .7                 |  |      |      | .31  | .34  | .40  | .41  |



TABLE III. Coefficients,  $d_i$ , resulting from the fit of the fatigue-crack growth data to the general second order equation:

| $S_{rms}$<br>ksi | $S_m$<br>ksi | $S_a$<br>ksi | R   | Coefficients $d_i$ of equation (31) |                      |                      |                      |                      |
|------------------|--------------|--------------|-----|-------------------------------------|----------------------|----------------------|----------------------|----------------------|
|                  |              |              |     | $d_1 \times 10^{-4}$                | $d_2 \times 10^{-4}$ | $d_3 \times 10^{-8}$ | $d_4 \times 10^{-8}$ | $d_5 \times 10^{-8}$ |
| 8.78             | 0            | 25           | -1  | 1.6725                              | -0.1652              | 2.8316               | -2.2420              | 0.5595               |
| 7.44             | 15           | 15           | 0   | 1.8361                              | -0.2112              | 3.2248               | -2.6680              | 0.6591               |
| 7.03             | 0            | 20           | -1  | -6.8010                             | -0.8149              | 36.011               | 48.942               | -10.309              |
| 5.76             | 20           | 10           | .33 | -1.8630                             | -2.0976              | -26.989              | 61.017               | -9.4048              |
| 5.27             | 0            | 15           | -1  |                                     |                      |                      |                      |                      |
| 5.24             | 22.5         | 7.5          | .33 | 11.573                              | 3.6700               | 178.56               | -97.553              | 66.816               |
| 4.96             | 10           | 10           | 0   | 3.7940                              | .21225               | 13.663               | -17.821              | 6.2801               |
| 4.71             | 30           | 5            | .7  | 25.987                              | -4.7535              | 491.25               | -443.08              | 103.24               |
| 4.36             | 18.75        | 6.25         | .5  | -290.97                             | -43.566              | 83310                | 31310                | 144.76               |
| 4.32             | 15           | 7.5          | .33 | 11.573                              | 3.6700               | 178.56               | -97.553              | 66.816               |
| 4.07             | 25           | 4.4          | .7  | -13.512                             | 2.0456               | -431.87              | 1459.6               | -414.32              |
| 3.72             | 7.5          | 7.5          | 0   | .14146                              | -9.9774              | -212.46              | 580.90               | -61.687              |
| 3.62             | 12.5         | 6.3          | .33 | 14.671                              | 1.3324               | 236.41               | -173.91              | 69.160               |
| 3.51             | 0            | 10           | -1  | -2.8132                             | -.39629              | 7.1794               | 20.718               | -5.6325              |
| 3.49             | 15           | 5            | .5  | 2.6306                              | -2.8775              | -58.161              | 204.65               | -50.856              |
| 3.24             | 20           | 3.5          | .7  | -58.485                             | 20.570               | 2291.7               | 5250.5               | -1890.9              |
| 2.88             | 10           | 5            | .33 | -1.6053                             | -2.7652              | -215.82              | 753.83               | -203.44              |
| 2.64             | 0            | 7.5          | -1  | -96.867                             | 4.4846               | 9365.8               | 8780.4               | -4280.9              |
| 2.62             | 11.25        | 3.25         | .5  | -22.243                             | 5.8944               | -119.07              | 3341.0               | -1043.3              |
| 2.48             | 5            | 5            | 0   | -1.60231                            | 2.6971               | -342.04              | 1274.7               | -363.60              |
| 2.42             | 15           | 2.6          | .7  | 422.52                              | -59.412              | 17120                | -134130              | 30988                |
| 1.86             | 3.75         | 3.75         | 0   | 455.81                              | -84.234              | 15380                | -147410              | 31133                |
| 1.75             | 7.5          | 2.5          | .5  | 490.34                              | -49.849              | 23900                | -223130              | 60111                |
| 1.44             | 5            | 2.5          | .33 | 2834.9                              | -122.69              | 8137100              | -1667500             | 318889               |
| 1.29             | 10           | 1.7          | .7  |                                     |                      |                      |                      |                      |





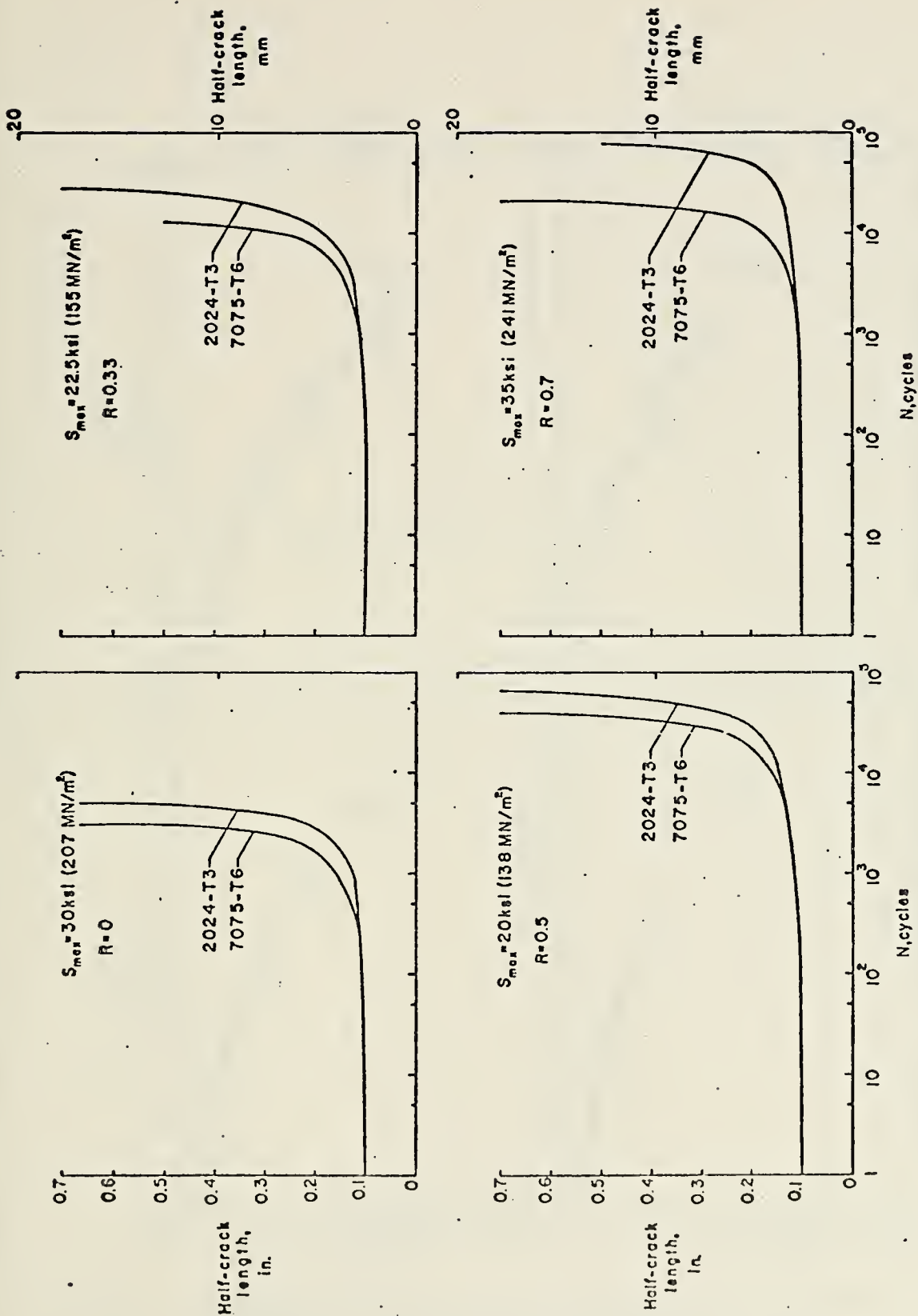


Figure 1. Typical fatigue-crack growth curves (from Ref. 1)





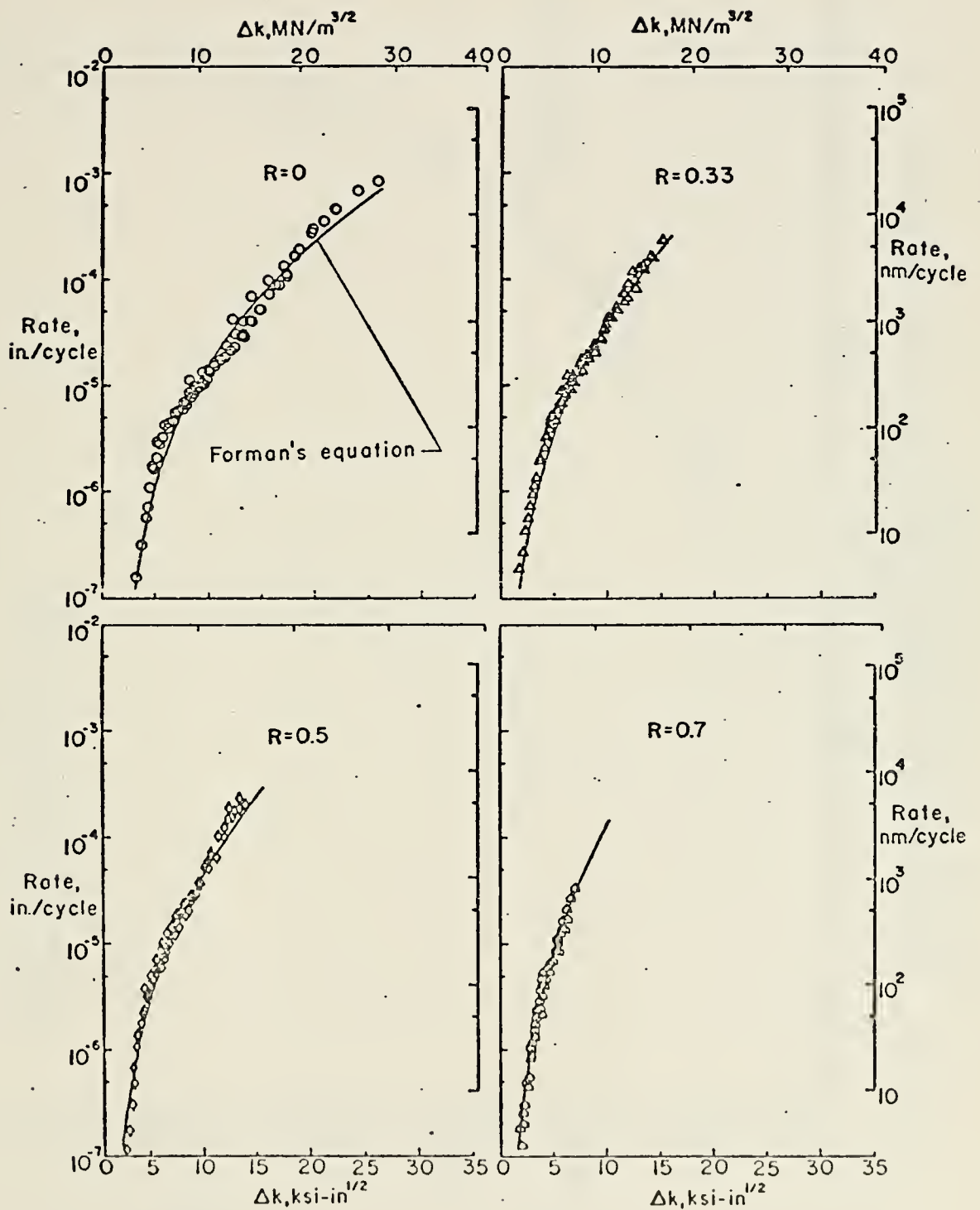


Figure 2. Hudson's comparison of fatigue-crack growth rate with Forman's equation (From Ref. 1).



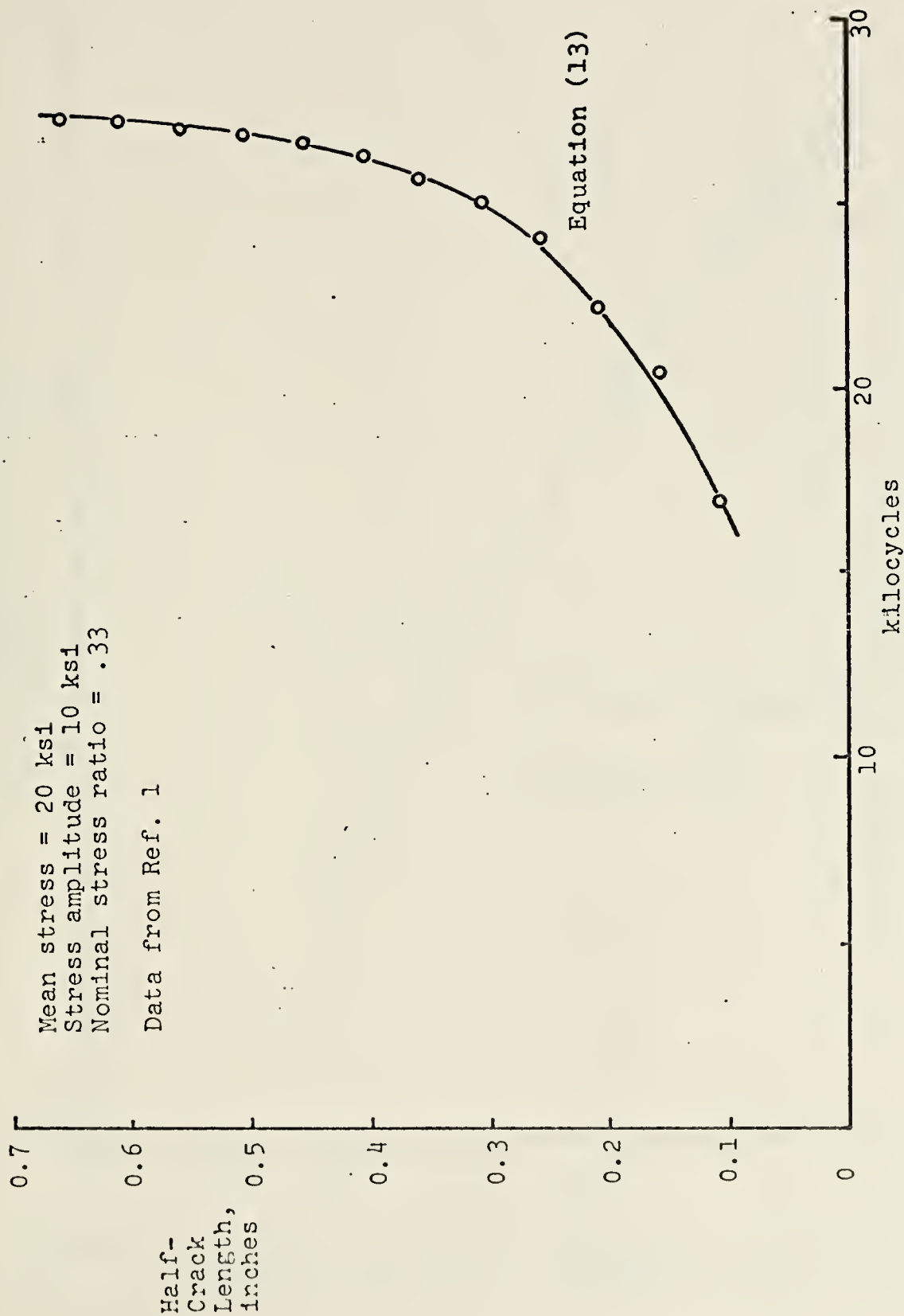


Figure 3. Comparison of a fatigue-crack growth curve with the power-rule prediction (typical).



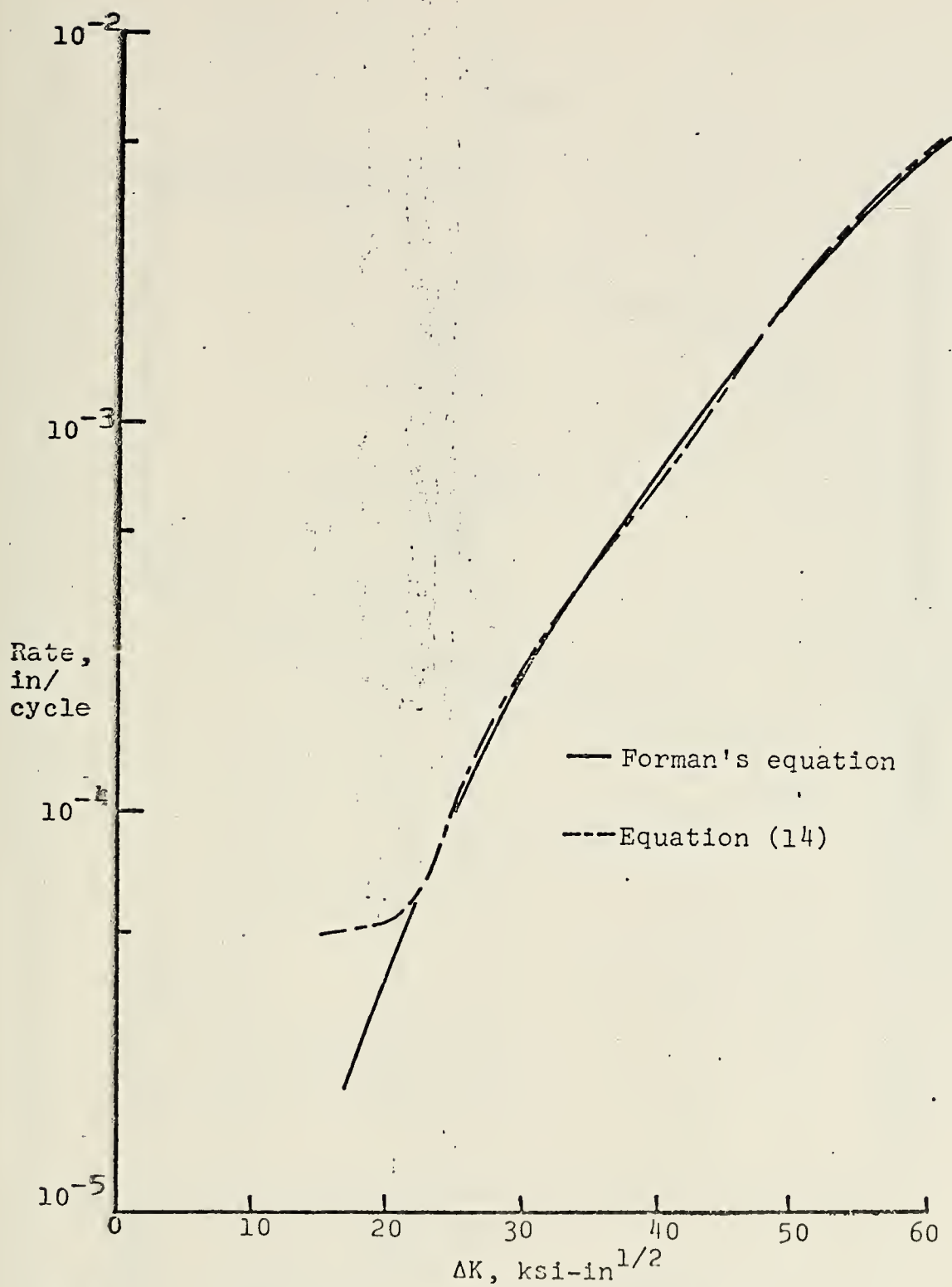


Figure 4. Comparison of fatigue-crack growth rate with Forman's equation for a single load case (typical).



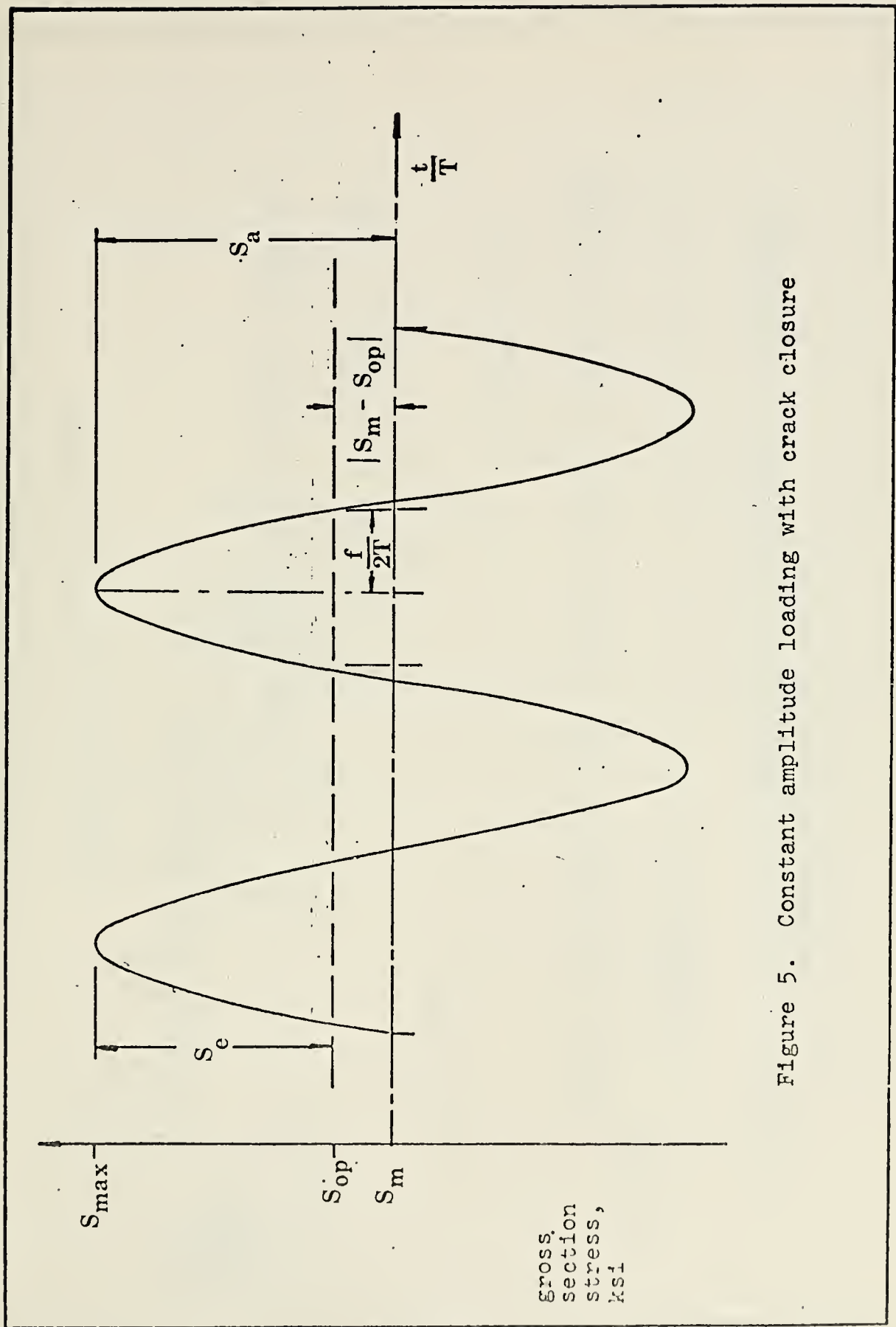


Figure 5. Constant amplitude loading with crack closure





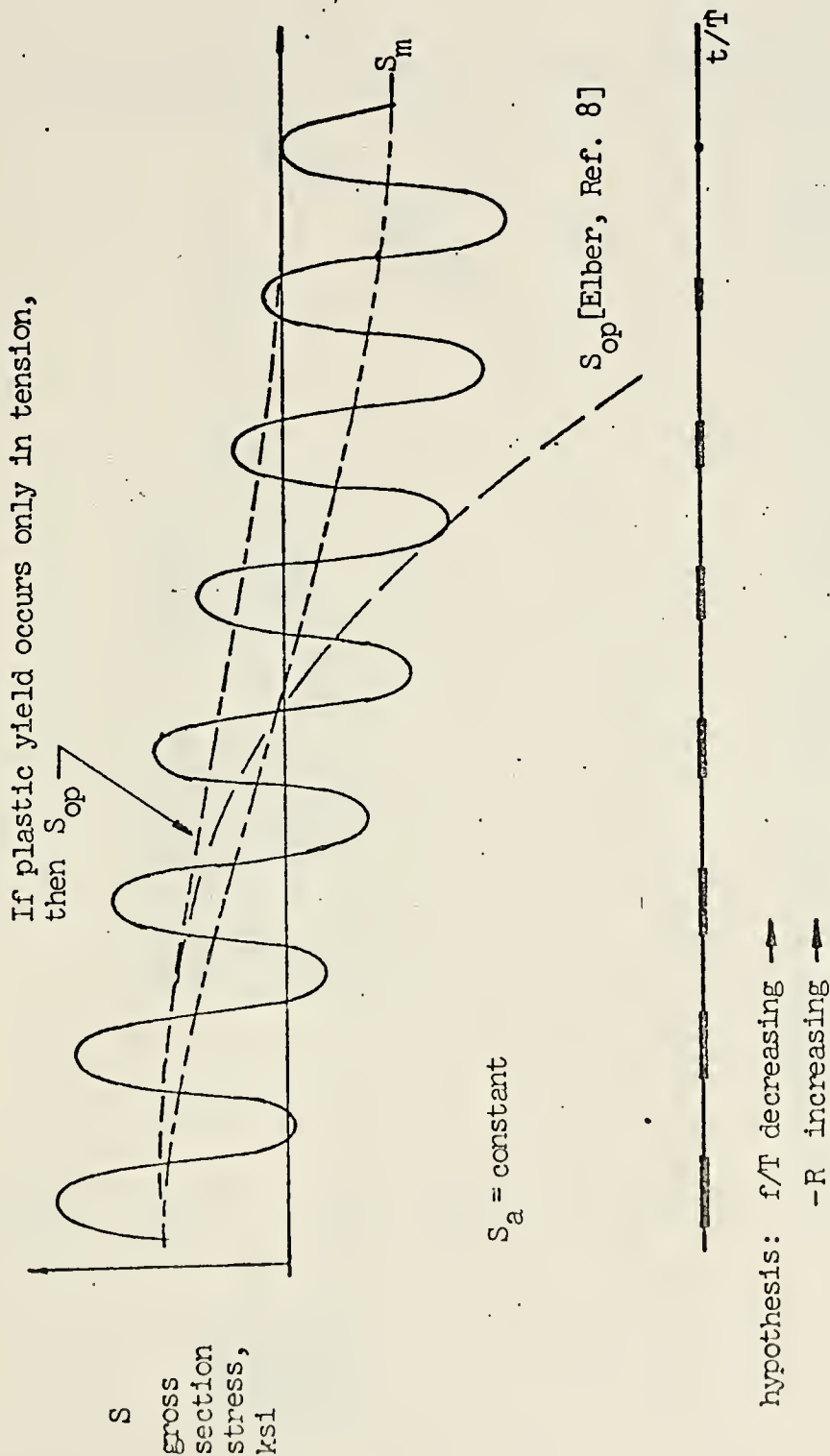


Figure 6. Schematic representation of the effect of increasingly negative cyclic stress ratios



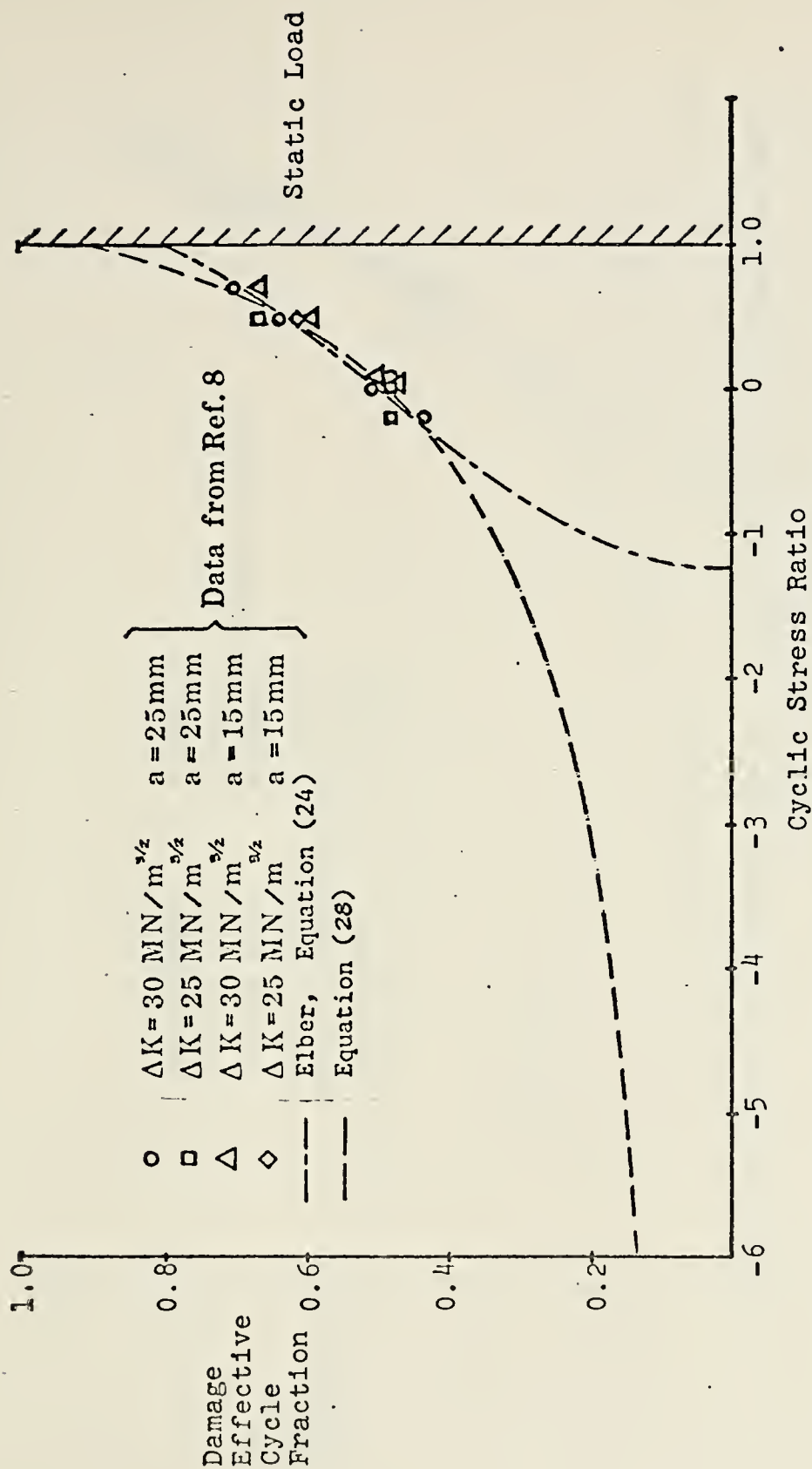


Figure 7. Variation of the damage effective cycle fraction with cyclic stress ratio.



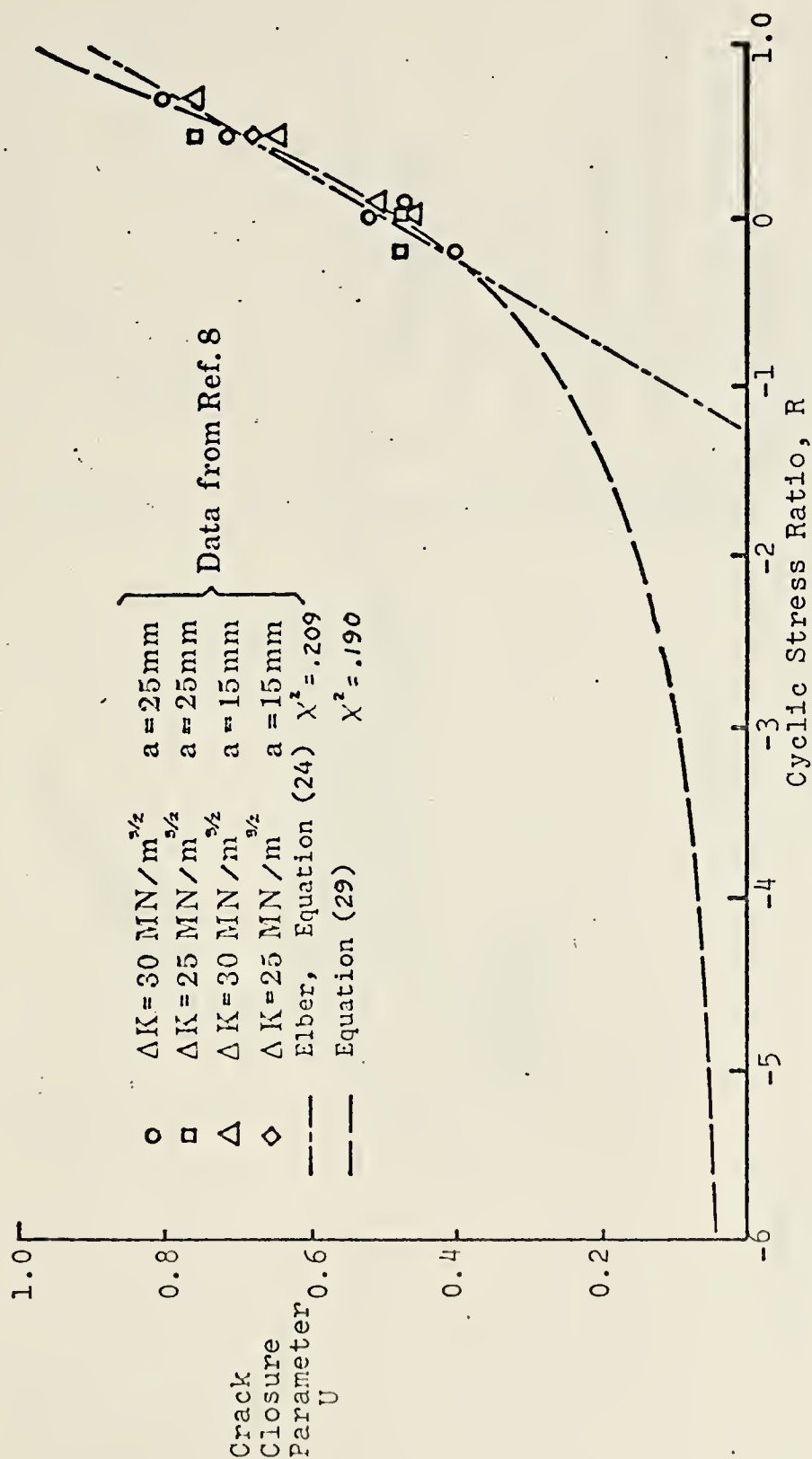
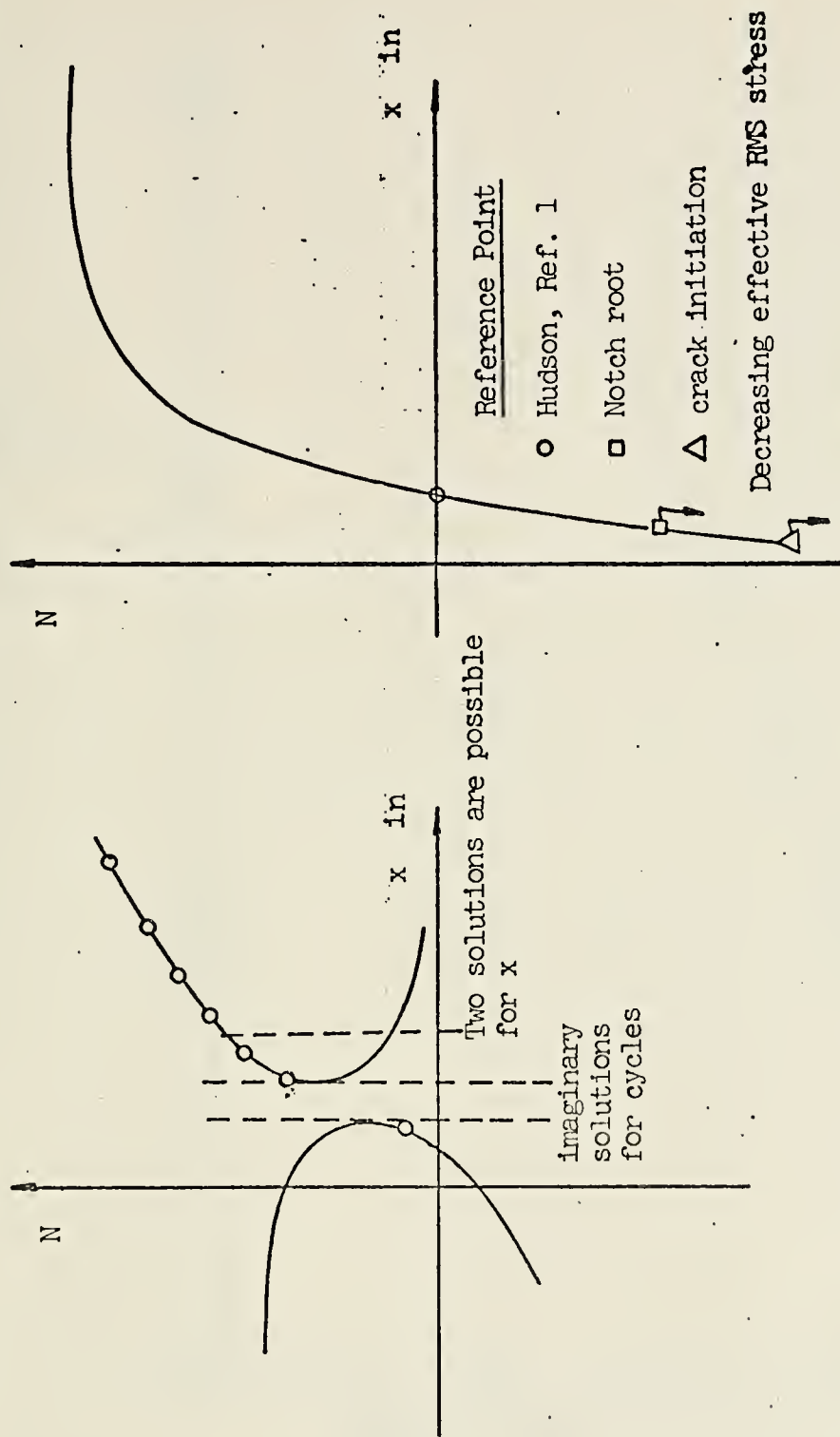


Figure 8. Comparison of two expressions for the crack-closure parameter





a) Parabolic

b) Hyperbolic

Figure 9. Geometric interpretation of the general second order polynomial fit to the fatigue-crack growth data.





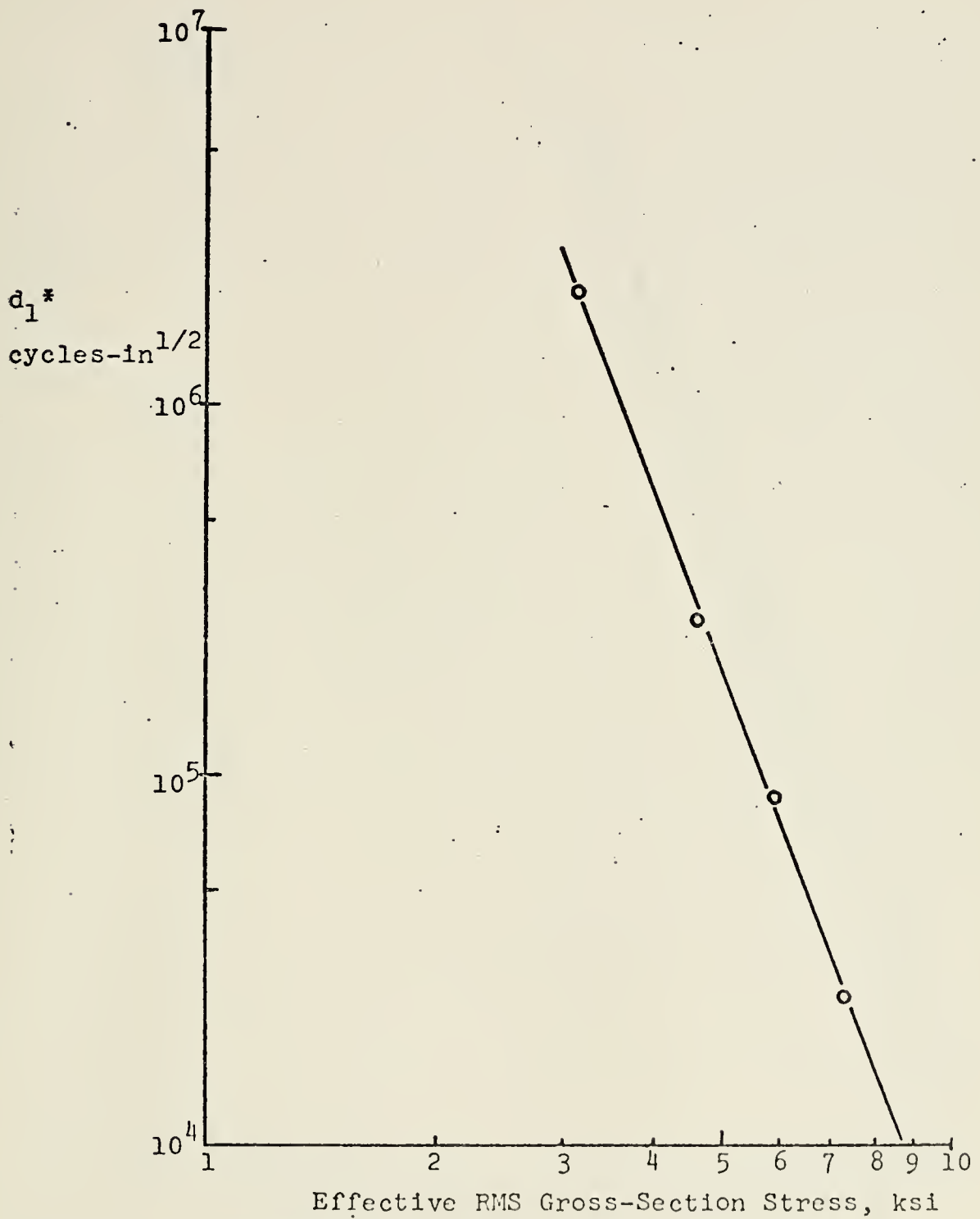


Figure 10. Correlation of the coefficient  $d_1^*$  with the effective RMS gross-section stress



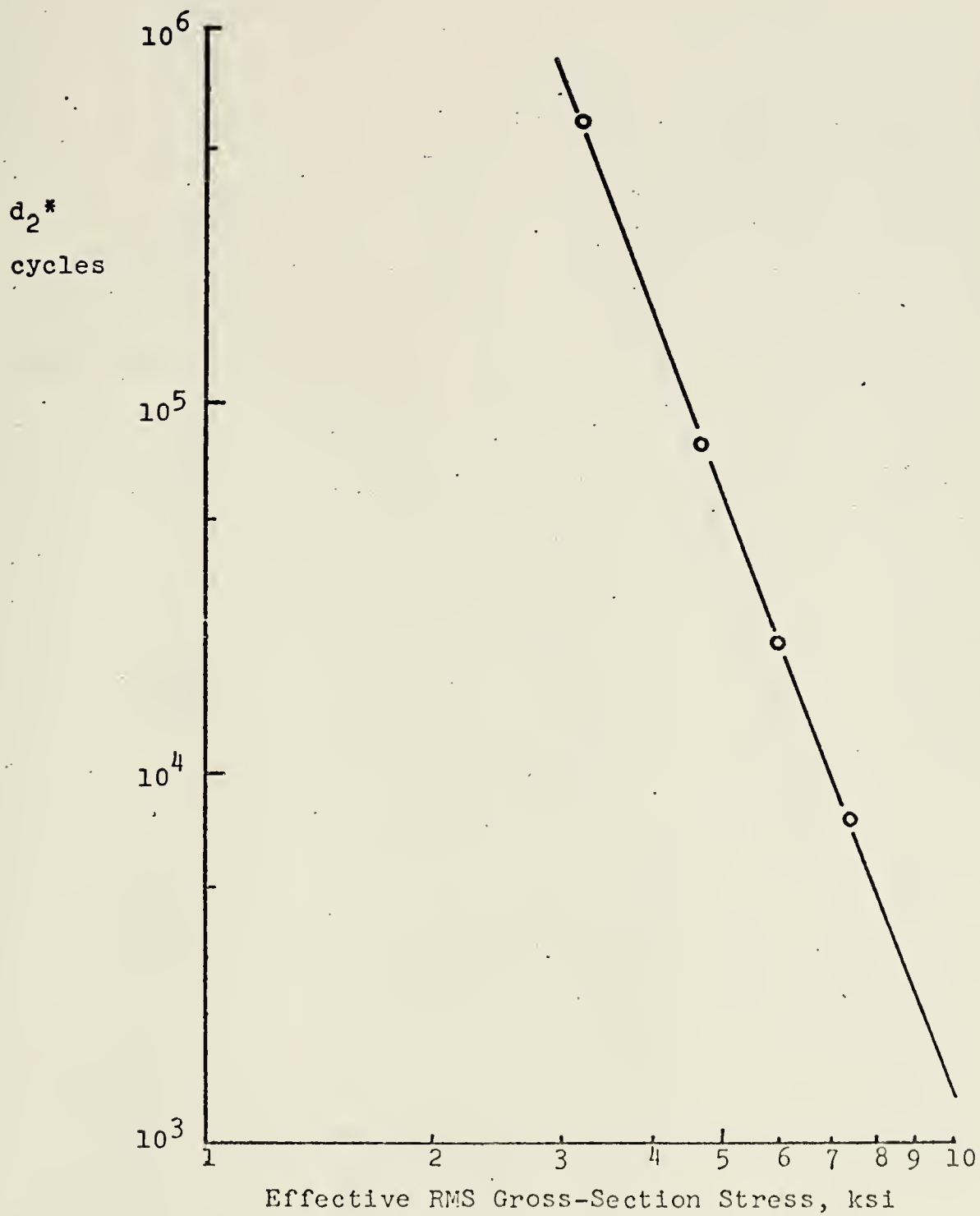


Figure 11. Correlation of the coefficient  $d_2^*$  with the effective RMS gross-section stress



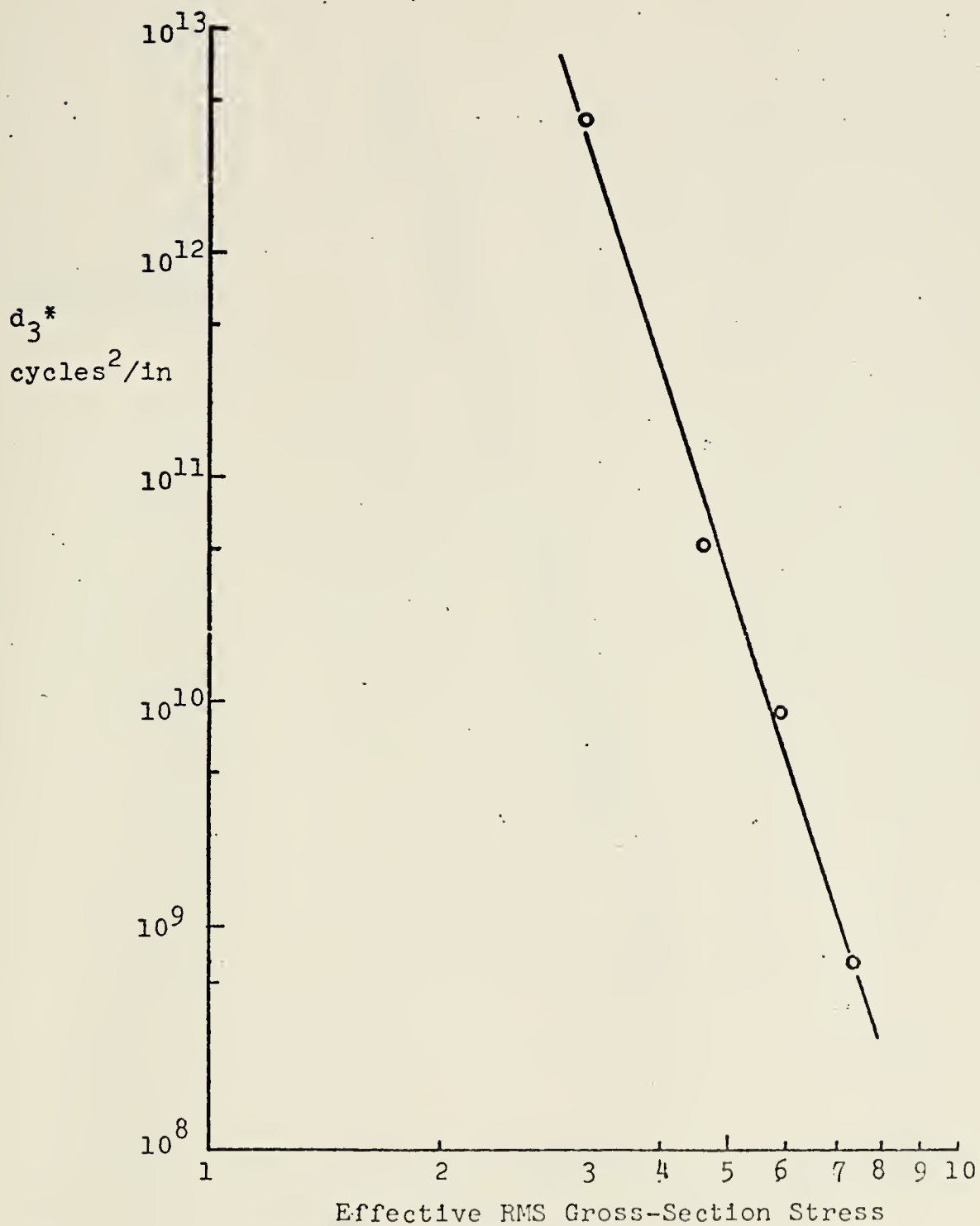


Figure 12. Correlation of the coefficient  $d_3^*$  with the effective RMS gross-section stress



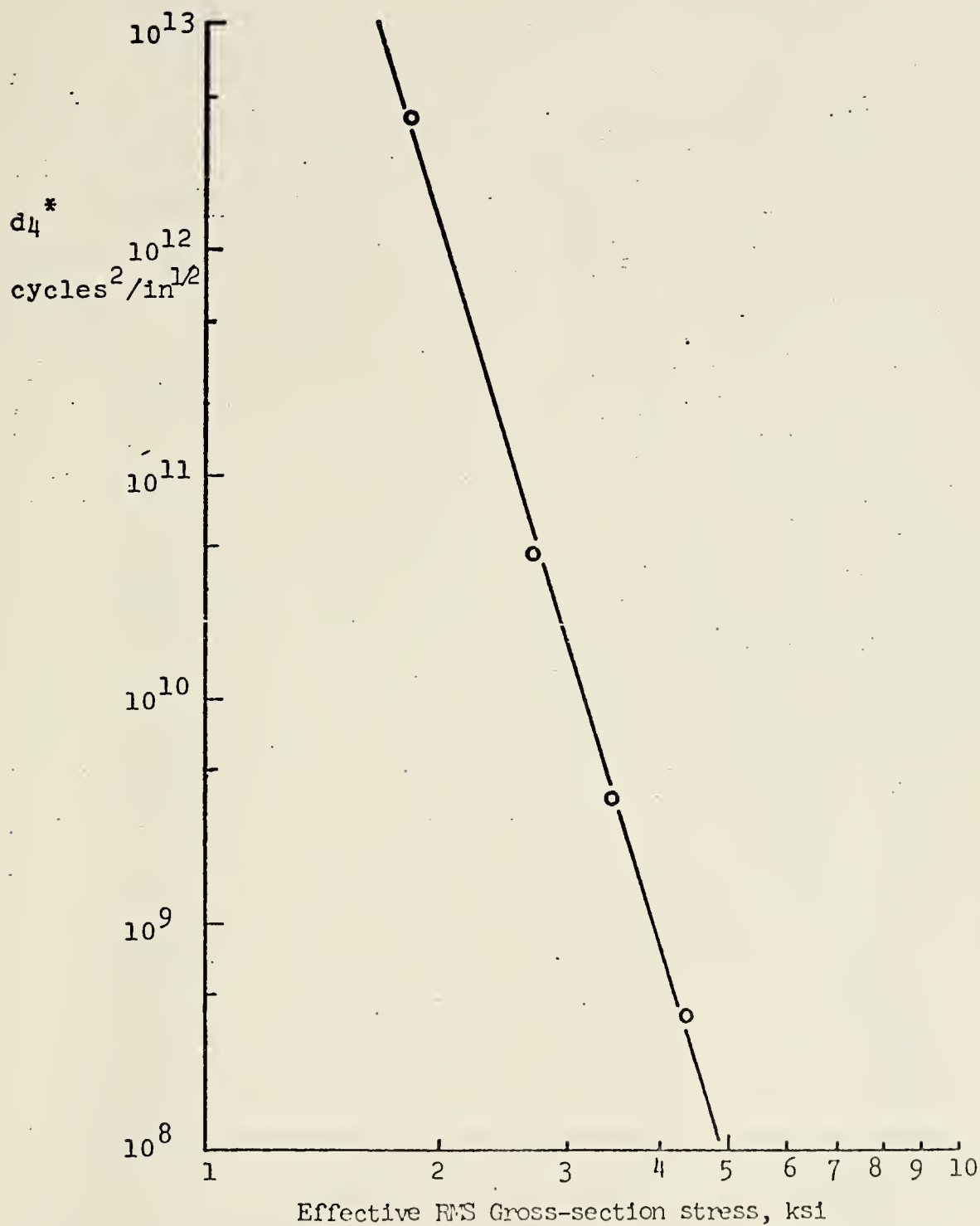


Figure 13. Correlation of the coefficient  $d_4^*$  with the effective RMS gross-section stress





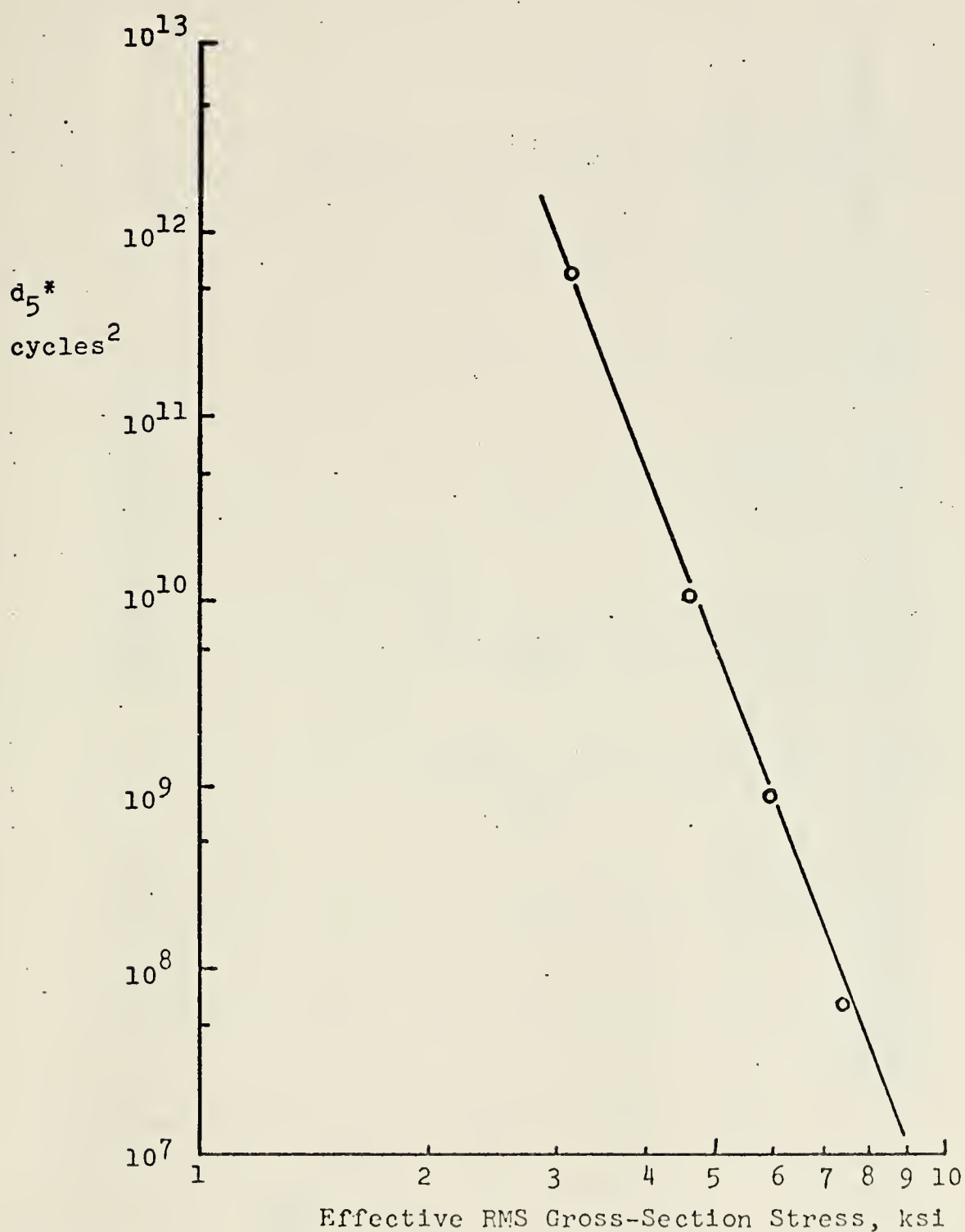


Figure 14. Correlation of the coefficient  $d_5^*$  with the effective RMS gross-section stress



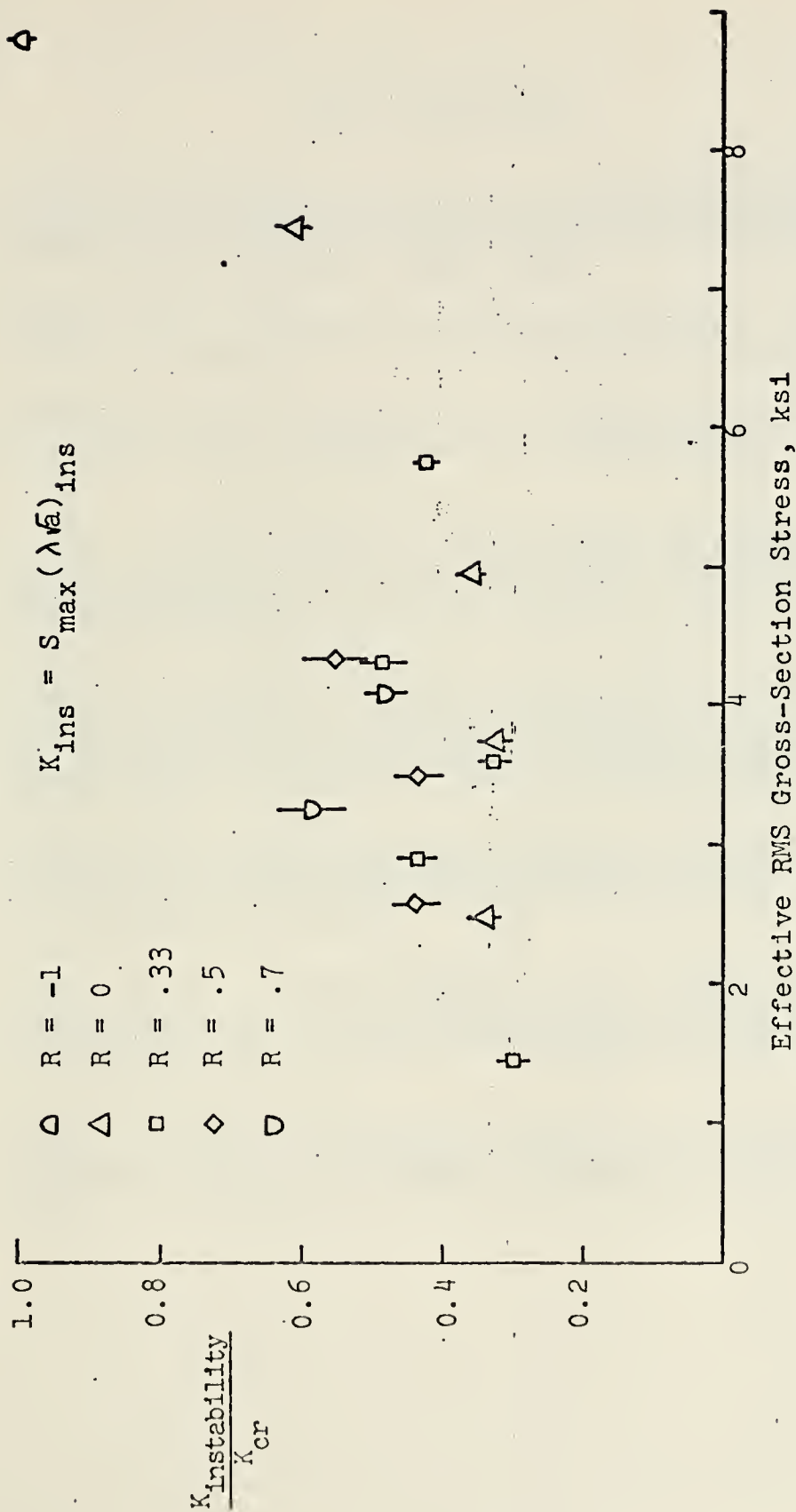


Figure 15. Relationship between the unstable crack propagation stress intensity factor and the effective RMS gross section stress



### LIST OF REFERENCES

1. National Aeronautics and Space Administration Technical Note D-5390, Effect of Stress Ratio on Fatigue-Crack Growth in 7075-T6 and 2024-T3 Aluminum-Alloy Specimens, by C. Michael Hudson, August 1969.
2. Miner, M. A., "Cumulative Damage in Fatigue," Journal of Applied Mechanics, v. 12, p. A159-A164, September 1945.
3. Walton, D. and Ellison, E. G., "Fatigue Crack Initiation and Propagation," International Metallurgical Reviews, v. 17, p. 100-116, 1972.
4. Paris, P. and Erdogan, F., "A Critical Analysis of Crack Propagation Laws," Transactions of the American Society of Mechanical Engineers, Ser. D: Journal of Basic Engineering, v. 85, p. 528-534, 1963.
5. Forman, R. G., Kearney, V. E., and Engle, R. M., "Numerical Analysis of Crack Propagation in Cyclic-Loaded Structures," Transactions of the American Society of Mechanical Engineers, Ser. D: Journal of Basic Engineering, v. 89, p. 459-464, September 1967.
6. Paris, P. C., "The Fracture Mechanics Approach to Fatigue," Fatigue, An Interdisciplinary Approach, edited by Burke, J. J., Reed, N. L., and Weiss, V., p. 107-132, Syracuse University Press, 1964.
7. Brown, W. F., Jr. and Srawley, J. E., Plane Strain Crack Toughness of High Strength Metallic Materials, ASTM STP 410, p. 11, American Society for Testing and Materials, 1966.
8. Elber, W., "The Significance of Fatigue Crack Closure," Damage Tolerance in Aircraft Structures, ASTM STP 486, p. 230-242, American Society for Testing and Materials, 1971.



INITIAL DISTRIBUTION LIST

|   | No. Copies |
|---|------------|
| 1. Defense Documentation Center<br>Cameron Station<br>Alexandria, Virginia 22314  | 2          |
| 2. Library, Code 0212<br>Naval Postgraduate School<br>Monterey, California 93940  | 2          |
| 3. Chairman<br>Department of Aeronautics<br>Naval Postgraduate School<br>Monterey, California 93940                                 | 1          |
| 4. Assoc. Professor G.H. Lindsey, Code 57Li<br>Department of Aeronautics<br>Naval Postgraduate School<br>Monterey, California 93940 | 2          |
| 5. National Aeronautics and Space Administration<br>Langley Research Center, Attn: MS 188E<br>Hampton, Virginia 23665               | 5          |
| 6. LT Robert Alan Kish<br>604 N. 68th Avenue<br>Pensacola, Florida 32506  | 2          |





Thesis

157036

K535 Kish

c.1

A critical analysis  
of fatigue-crack pro-  
pagation data for 2024-  
T3 aluminum.

Thesis

157036

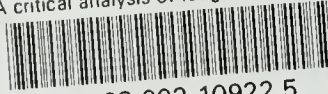
K535 Kish

c.1

A critical analysis  
of fatigue-crack pro-  
pagation data for 2024-  
T3 aluminum.

thesK535

A critical analysis of fatigue-crack pro



3 2768 002 10922 5

DUDLEY KNOX LIBRARY